



CMS-SUS-10-009

CERN-PH-EP/2011-099
2011/07/08

Inclusive search for squarks and gluinos in pp collisions at $\sqrt{s} = 7 \text{ TeV}$

The CMS Collaboration^{*}

Abstract

A search is performed for heavy particle pairs produced in $\sqrt{s} = 7 \text{ TeV}$ proton-proton collisions with 35 pb^{-1} of data collected by the CMS experiment at the LHC. The search is sensitive to squarks and gluinos of generic supersymmetry models, provided they are kinematically accessible, with minimal assumptions on properties of the lightest superpartner particle. The kinematic consistency of the selected events is tested against the hypothesis of heavy particle pair production using the dimensionless *razor* variable R , related to the missing transverse energy E_T^{miss} . The new physics signal is characterized by a broad peak in the distribution of M_R , an event-by-event indicator of the heavy particle mass scale. This new approach is complementary to E_T^{miss} -based searches. After background modeling based on data, and background rejection based on R and M_R , no significant excess of events is found beyond the standard model expectations. The results are interpreted in the context of the constrained minimal supersymmetric standard model as well as two simplified supersymmetry models.

Submitted to Physical Review D

^{*}See Appendix A for the list of collaboration members

1 Introduction

Models with softly broken supersymmetry (SUSY) [1–5] predict superpartners of the standard model (SM) particles. Experimental limits from the Tevatron and LEP showed that superpartner particles, if they exist, are significantly heavier than their SM counterparts. Proposed experimental searches for R -parity conserving SUSY at the Large Hadron Collider (LHC) have therefore focused on a combination of two SUSY signatures: multiple energetic jets and/or leptons from the decays of pair-produced squarks and gluinos, and large missing transverse energy (E_T^{miss}) from the two weakly interacting lightest superpartners (LSP) produced in separate decay chains.

In this article a new approach is presented that is inclusive not only for SUSY but also in the larger context of physics beyond the standard model. The focal point for this novel *razor* analysis [6] is the production of pairs of heavy particles (of which squarks and gluinos are examples), whose masses are significantly larger than those of any SM particle. The analysis is designed to kinematically discriminate the pair production of heavy particles from SM backgrounds, without making strong assumptions about the E_T^{miss} spectrum or details of the decay chains of these particles. The baseline selection requires two or more reconstructed objects, which can be calorimetric jets, isolated electrons or isolated muons. These objects are grouped into two *megajets*. The razor analysis tests the consistency, event by event, of the hypothesis that the two megajets represent the visible portion of the decays of two heavy particles. This strategy is complementary to traditional searches for signals in the tails of the E_T^{miss} distribution [7–16] and is applied to data collected with the Compact Muon Solenoid (CMS) detector from pp collisions at $\sqrt{s} = 7 \text{ TeV}$ corresponding to an integrated luminosity of 35 pb^{-1} .

2 The CMS Apparatus

A description of the CMS detector can be found elsewhere [17]. A characteristic feature of the CMS detector is its superconducting solenoid magnet, of 6 m internal diameter, providing a field of 3.8 T. The silicon pixel and strip tracker, the crystal electromagnetic calorimeter (ECAL) and the brass/scintillator hadron calorimeter (HCAL) are contained within the solenoid. Muons are detected in gas-ionization chambers embedded in the steel return yoke. The ECAL has an energy resolution of better than 0.5 % above 100 GeV. The HCAL combined with the ECAL, measures the jet energy with a resolution $\Delta E/E \approx 100\%/\sqrt{E/\text{GeV}} \oplus 5\%$.

CMS uses a coordinate system with the origin located at the nominal collision point, the x -axis pointing towards the center of the LHC, the y -axis pointing up (perpendicular to the LHC plane), and the z -axis along the counterclockwise beam direction. The azimuthal angle ϕ is measured with respect to the x -axis in the xy plane and the polar angle θ is defined with respect to the z -axis. The pseudorapidity is $\eta = -\ln[\tan(\theta/2)]$.

3 The Razor Analysis

The pair production of two heavy particles, each decaying to an unseen LSP plus jets, gives rise to a generic SUSY-like signal. Events in this analysis are forced into a dijet topology by combining all jets in the event into two megajets. When an isolated lepton is present, it can be included in the megajets or not, as described in Sections 4 and 5. To the extent that the pair of megajets accurately reconstructs the visible portion of the underlying parent particle decays, the kinematic properties of the signal are equivalent to the pair production of, for example, two heavy squarks \tilde{q}_1, \tilde{q}_2 , with $\tilde{q}_i \rightarrow j_i \tilde{\chi}_i^0$, for $i = 1, 2$, where j_i and $\tilde{\chi}_i^0$ denote the visible and

invisible products of the decays, respectively. In the approximation that the heavy squarks are produced at threshold and their visible decay products are massless, the center of mass (CM) frame four-momenta are

$$p_{j_1} = \frac{M_\Delta}{2}(1, \hat{u}_1), \quad p_{j_2} = \frac{M_\Delta}{2}(1, \hat{u}_2), \quad (1)$$

$$p_{\tilde{\chi}_1} = \frac{M_\Delta}{2} \left(\frac{2M_{\tilde{q}}}{M_\Delta} - 1, -\hat{u}_1 \right), \quad p_{\tilde{\chi}_2} = \frac{M_\Delta}{2} \left(\frac{2M_{\tilde{q}}}{M_\Delta} - 1, -\hat{u}_2 \right), \quad (2)$$

where \hat{u}_i is the unit vector in the direction of j_i , and

$$M_\Delta \equiv \frac{M_{\tilde{q}}^2 - M_{\tilde{\chi}}^2}{M_{\tilde{q}}}, \quad (3)$$

where $M_{\tilde{q}}$ and $M_{\tilde{\chi}}$ are the squark and LSP masses, respectively.

In events with two undetected particles in the partonic final state, it is not possible to reconstruct the actual CM frame. Instead, an approximate event-by-event reconstruction is made assuming the dijet signal topology, replacing the CM frame with the *R frame* [6], defined as the longitudinally boosted frame that equalizes the magnitude of the two megajets' three-momenta. The *R* frame would be the CM frame for signal events, if the squarks were produced at threshold and if the CM system had no overall transverse momentum from initial-state radiation. The longitudinal Lorentz boost factor is defined by

$$\beta_R \equiv \frac{E^{j_1} - E^{j_2}}{p_z^{j_1} - p_z^{j_2}}, \quad (4)$$

where E^{j_1} , E^{j_2} and $p_z^{j_1}$, $p_z^{j_2}$ are the megajet energies and longitudinal momenta, respectively. To the extent that the *R* frame matches the true CM frame, the maximum value of the scalar sum of the megajets' transverse momenta (p_T^1 , p_T^2) is M_Δ for signal events. The maximum value of the E_T^{miss} is also M_Δ . A transverse mass M_T^R is defined whose maximum value for signal events is also M_Δ in the limit that the *R* and CM frames coincide:

$$M_T^R \equiv \sqrt{\frac{E_T^{\text{miss}}(p_T^{j_1} + p_T^{j_2}) - \vec{E}_T^{\text{miss}} \cdot (\vec{p}_T^{j_1} + \vec{p}_T^{j_2})}{2}}. \quad (5)$$

The event-by-event estimator of M_Δ is

$$M_R \equiv 2|\vec{p}_{j_1}^R| = 2|\vec{p}_{j_2}^R|, \quad (6)$$

where $\vec{p}_{j_1}^R$ and $\vec{p}_{j_2}^R$ are the 3-momenta of the megajets in the *R* frame. For signal events in the limit where the *R* frame and the true CM frame coincide, M_R equals M_Δ , and more generally M_R is expected to peak around M_Δ for signal events. For QCD dijet and multijet events the only relevant scale is $\sqrt{\hat{s}}$, the CM energy of the partonic subprocess. The search for an excess of signal events in a tail of a distribution is thus recast as a search for a peak on top of a steeply falling SM residual tail in the M_R distribution. To extract the peaking signal, the QCD multijet

background needs to be reduced to manageable levels. This is achieved using the *razor* variable defined as:

$$R \equiv \frac{M_T^R}{M_R} . \quad (7)$$

Since for signal events M_T^R has a maximum value of M_Δ (i.e., a kinematic edge), R has a maximum value of approximately 1 and the distribution of R for signal events peaks around 0.5. These properties motivate the appropriate kinematic requirements for the signal selection and background reduction. It is noted that, while M_T^R and M_R measure the same scale (one as an end-point, the other as a peak), they are largely uncorrelated for signal events, as shown in Fig. 1. In this figure, the $W+jets$ and $t\bar{t}+jets$ backgrounds peak at M_R values partially determined by the W and top quark masses, respectively.

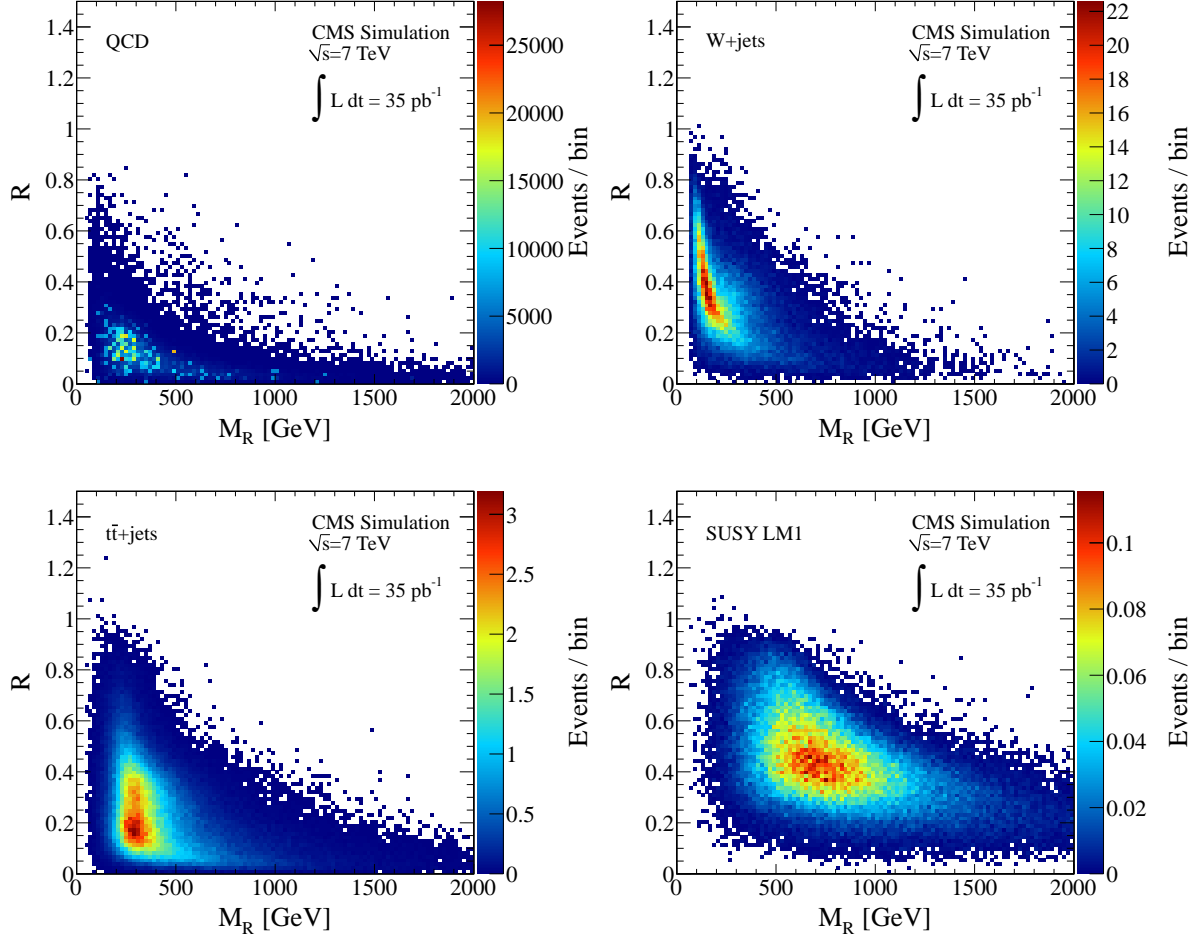


Figure 1: Scatter plot in the (M_R, R) plane for simulated events: (top left) QCD multijet, (top right) $W+jets$, (bottom left) $t\bar{t}+jets$, and (bottom right) the SUSY benchmark model LM1 [18] with $M_\Delta = 597$ GeV. The yields are normalized to an integrated luminosity of 35 pb^{-1} . The bin size is $(20 \text{ GeV} \times 0.015)$.

In this analysis the SM background shapes and normalizations are obtained from data. The backgrounds are extracted from control regions in the R and M_R distributions dominated by SM processes. Initial estimates of the background distributions in these regions are obtained

from the individual simulated background components, but their shapes and normalizations are then corrected using data. The analysis flow is as follows:

1. The inclusive data sets are collected using the electron, muon, and hadronic-jet triggers.
2. These data sets are examined for the presence of a well-identified isolated electron or muon, irrespective of the trigger path. Based on the presence or absence of such a lepton, each event is assigned to one of three disjoint event samples, referred to as the electron, muon, and hadronic *boxes*. These boxes serve as controls of processes in the SM with leptons, jets, and neutrinos, e.g. QCD multijet, $W+jets$ or $Z+jets$, and $t+X$. The diboson background is found to be negligible. Exclusive multilepton boxes are also defined but are not sufficiently populated to be used in this analysis.
3. Megajets are constructed for events passing a baseline kinematic selection, and the R and M_R event variables are computed. In the electron box, electrons are clustered with jets in the definition of the megajets. Jets matched to these electrons are removed to avoid double-counting. In the muon box, muons are included in the megajet clustering.
4. In order to characterize the distribution of the SM background events in the (M_R , R) plane, a kinematic region is identified in the lepton boxes that is dominated by $W(\ell\nu)+jets$. Another region is found that is dominated by the sum of the non-QCD backgrounds.
5. Events remaining in the hadronic box primarily consist of QCD multijet, $Z(\nu\bar{\nu})+jets$, $W(\ell\nu)+jets$, and $t+X$ events that produce $\ell+jets+E_T^{\text{miss}}$ final states with charged leptons that do not satisfy the electron or muon selections. The shapes and normalizations of these non-QCD background processes in the hadronic box are estimated using the results from the lepton boxes in appropriate regions in the (M_R , R) plane.
6. The QCD background shape and normalization in each of the lepton boxes is extracted by reversing the lepton isolation requirements to obtain control samples dominated by QCD background.
7. The QCD background in the hadronic box is estimated using QCD control samples collected with prescaled jet triggers.
8. The large- R and high- M_R regions of all boxes are signal candidate regions not used for the background estimates. Above a given R threshold, the M_R distribution of the backgrounds observed in the data is well modeled by simple exponential functions. Having determined the R and M_R shape and normalization of the backgrounds in the control regions, the SM yields are extrapolated to the large- R and high- M_R signal candidate regions for each box.

4 Event Selection

The analysis uses data sets recorded with triggers based on the presence of an electron, a muon, or on H_T , the uncorrected scalar sum of the transverse energy of jets reconstructed at the trigger level. Prescaled jet triggers with low thresholds are used for the QCD multijet background estimation in the hadronic box.

The analysis is guided by studies of Monte Carlo (MC) event samples generated with the PYTHIA [19] and MADGRAPH [20] programs, simulated using the CMS GEANT-based [21] detector simulation, and then processed by the same software used to reconstruct real collision

data. Events with QCD multijet, top quarks, and electroweak bosons were generated with MADGRAPH interfaced with PYTHIA for parton showering, hadronization, and underlying event description. To generate Monte Carlo samples for SUSY, the mass spectrum was first calculated with SOFTSUSY [22] and the decays with SUSYHIT [23]. The PYTHIA program was used with the SLHA interface [24] to generate the events. The generator level cross section and the K factors for the next-to-leading order (NLO) cross section calculation were computed using PROSPINO [25].

Events are required to have at least one good reconstructed interaction vertex [26]. When multiple vertices are found, the one with the highest associated $\sum_{\text{track}} p_T$ is used. Jets are reconstructed offline from calorimeter energy deposits using the infrared-safe anti- k_T [27] algorithm with radius parameter 0.5. Jets are corrected for the nonuniformity of the calorimeter response in energy and η using corrections derived with the simulation and are required to have $p_T > 30 \text{ GeV}$ and $|\eta| < 3.0$. The jet energy scale uncertainty for these corrected jets is 5% [28]. The E_T^{miss} is reconstructed using the particle flow algorithm [29].

The electron and muon reconstruction and identification criteria are described in [30]. Isolated electrons and muons are required to have $p_T > 20 \text{ GeV}$ and $|\eta| < 2.5$ and 2.1, respectively, and to satisfy the selection requirements from [30]. The typical lepton trigger and reconstruction efficiencies are 98% and 99%, respectively, for electrons and 95% and 98% for muons.

The reconstructed hadronic jets, isolated electrons, and isolated muons are grouped into two megajets, when at least two such objects are present in the event. The megajets are constructed as a sum of the four-momenta of their constituent objects. After considering all possible partitions of the objects into two megajets, the combination minimizing the invariant masses summed in quadrature of the resulting megajets is selected among all combinations for which the R frame is well defined.

After the construction of the two megajets the boost variable $|\beta_R|$ is computed; due to the approximations mentioned above, $|\beta_R|$ can fall in an unphysical region (≥ 1) for signal or background events; these events are removed. The additional requirement $|\beta_R| \leq 0.99$ is imposed to remove events for which the razor variables become singular. This requirement is typically 85% efficient for simulated SUSY events. The azimuthal angular difference between the megajets is required to be less than 2.8 radians; this requirement suppresses nearly back-to-back QCD di-jet events. These requirements define the inclusive baseline selection. After this selection, the signal efficiency in the constrained minimal supersymmetric standard model (CMSSM) [31–34] parameter space for a gluino mass of $\sim 600 \text{ GeV}$ is over 50%.

5 Background Estimation

In traditional searches for SUSY based on missing transverse energy, it is difficult to model the tails of the E_T^{miss} distribution and the contribution from events with spurious instrumental effects. The QCD multijet production is an especially daunting background because of its very high cross section and complicated modeling of its high- p_T and E_T^{miss} tails. In this analysis a cut on R makes it possible to isolate the QCD multijet background in the low- M_R region.

Apart from QCD multijet backgrounds, the remaining backgrounds in the lepton and hadronic boxes are processes with genuine E_T^{miss} due to energetic neutrinos and leptons from massive vector boson decays (including W bosons from top quark decays). After applying an R threshold, the M_R distributions in the lepton and hadronic boxes are very similar for these backgrounds; this similarity is exploited in the modeling and normalization of these backgrounds.

5.1 QCD multijet background

The QCD multijet control sample for the hadronic box is defined from event samples recorded with prescaled jet triggers and passing the baseline analysis selection for events without a well-identified isolated electron or muon. The trigger requires at least two jets with an average uncorrected $p_T > 15 \text{ GeV}$. Because of the low jet threshold, the QCD multijet background dominates this sample for low M_R , thus allowing the extraction of the M_R shapes with different R thresholds for QCD multijet events. These shapes are corrected for the H_T trigger turn-on efficiency.

The M_R distributions for events satisfying the QCD control box selection, for different values of the R threshold, are shown in Fig. 2 (left). The M_R distribution is exponentially falling, after a turn-on at low M_R resulting from the p_T threshold requirement on the jets entering the megajet calculation. After the turn-on which is fitted with an asymmetric Gaussian, the exponential region of these distributions is fitted for each value of R to extract the exponential slope, denoted by S . The value of S that maximizes the likelihood in the exponential fit is found to be a linear function of R^2 , as shown in Fig. 2 (right); fitting S to the form $S = a + bR^2$ determines the values of a and b .

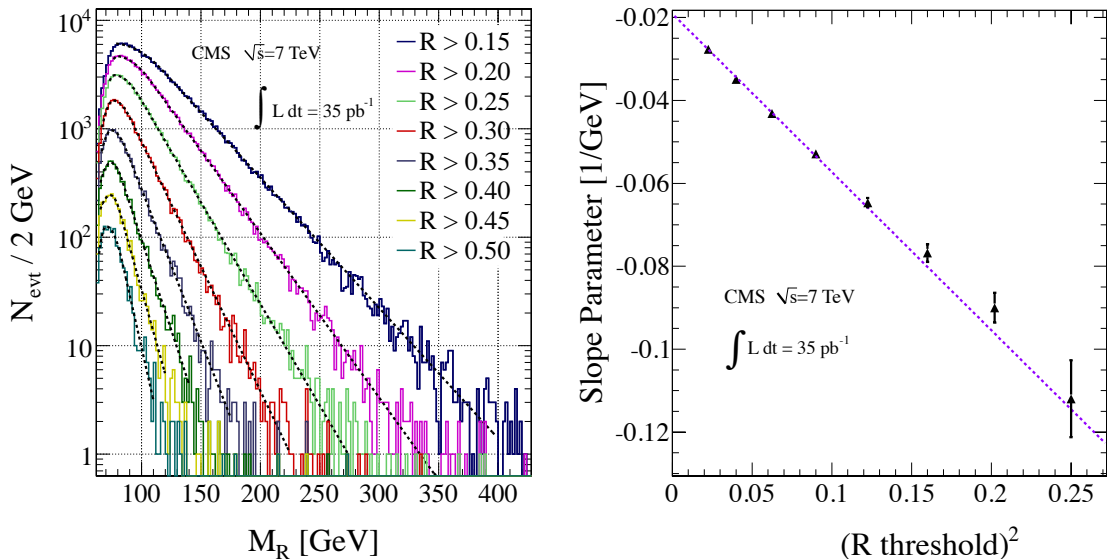


Figure 2: (Left) M_R distributions for different values of the R threshold for data events in the QCD control box. Fits of the M_R distribution to an exponential function and an asymmetric Gaussian at low M_R , are shown as dotted black curves. (Right) The exponential slope S from fits to the M_R distribution, as a function of the square of the R threshold for data events in the QCD control box.

When measuring the exponential slopes of the M_R distributions as a function of the R threshold, the correlations due to events satisfying multiple R threshold requirements are neglected. The effect of these correlations on the measurement of the slopes is studied by using pseudo-experiments and is found to be negligible.

To measure the shape of the QCD background component in the lepton boxes, the corresponding lepton trigger data sets are used with the baseline selection and reversed lepton isolation criteria. The QCD background component in the lepton boxes is found to be negligible.

The R threshold shapes the M_R distribution in a simple therefore predictable way. Event selections with combined R and M_R thresholds are found to suppress jet mismeasurements, including severe mismeasurements of the electromagnetic or hadronic component of the jet energy, or other anomalous calorimetric noise signals such as the ones described in [35, 36].

5.2 W+jets, Z+jets, and t+X backgrounds

Using the muon (MU) and electron (ELE) control boxes defined in Section 3, M_R intervals dominated by $W(\ell\nu)$ +jets events are identified for different R thresholds. In both simulated and data events, the M_R distribution is well described by two independent exponential components. The first component of $W(\ell\nu)$ +jets corresponds to events where the highest p_T object in one of the megajets is the isolated electron or muon; the second component consists of events where the leading object in both megajets is a jet, as is typical also for the $t+X$ background events. The first component of $W(\ell\nu)$ +jets can be measured directly in data, because it dominates over all other backgrounds in a control region of lower M_R set by the R threshold. At higher values of M_R , the first component of $W(\ell\nu)$ +jets falls off rapidly, and the remaining background is instead dominated by the sum of $t+X$ and the second component of $W(\ell\nu)$ +jets; this defines a second control region of intermediate M_R set by the R threshold.

Using these two control regions in a given box, a simultaneous fit determines both exponential slopes along with the absolute normalization of the first component of $W(\ell\nu)$ +jets and the relative normalization of the sum of the second component of $W(\ell\nu)$ +jets with the other backgrounds. The M_R distributions as a function of R are shown in Fig. 3 (left). The slope parameters characterizing the exponential behavior of the first $W(\ell\nu)$ +jets component are shown in Fig. 3 (right); they are consistent within uncertainties between the electron and muon channels. The values of the parameters a and b that describe the R^2 dependence of the slope are in good agreement with the values extracted from simulated $W(\ell\nu)$ +jets events.

The data/MC ratios $\rho(a)_1^{\text{data}/\text{MC}}$, $\rho(b)_1^{\text{data}/\text{MC}}$ of the first component slope parameters a, b measured in the MU and ELE boxes are thus combined yielding

$$\rho(a)_1^{\text{data}/\text{MC}} = 0.97 \pm 0.02 ; \quad \rho(b)_1^{\text{data}/\text{MC}} = 0.97 \pm 0.02 , \quad (8)$$

where the quoted uncertainties are determined from the fits.

The ratios $\rho^{\text{data}/\text{MC}}$ are taken as correction factors for the shapes of the Z +jets and $t+X$ backgrounds as extracted from simulated samples for the MU and ELE boxes; the same corrections are used for the shape of the first component of $W(\ell\nu)$ +jets as extracted from simulated samples for the hadronic (HAD) box.

The data/MC correction factors for the $Z(\nu\bar{\nu})$ +jets and $t+X$ backgrounds in the HAD box, as well as the second component of $W(\ell\nu)$ +jets in the MU, ELE, and HAD boxes, are measured in the MU and ELE boxes using a *lepton-as-neutrino* treatment of leptonic events. Here the electron or muon is excluded from the megajet reconstruction, kinematically mimicking the presence of an additional neutrino. With the lepton-as-neutrino treatment in the MU and ELE boxes only one exponential component is observed both in data and in $W(\ell\nu)$ +jets simulated events. In the simulation, the value of this single exponential component slope is found to agree with the value for the second component of $W(\ell\nu)$ +jets obtained in the default treatment.

The combined data/MC correction factors measured using this lepton-as-neutrino treatment are

$$\rho(a)_2^{\text{data}/\text{MC}} = 1.01 \pm 0.02 ; \quad \rho(b)_2^{\text{data}/\text{MC}} = 0.94 \pm 0.07 . \quad (9)$$

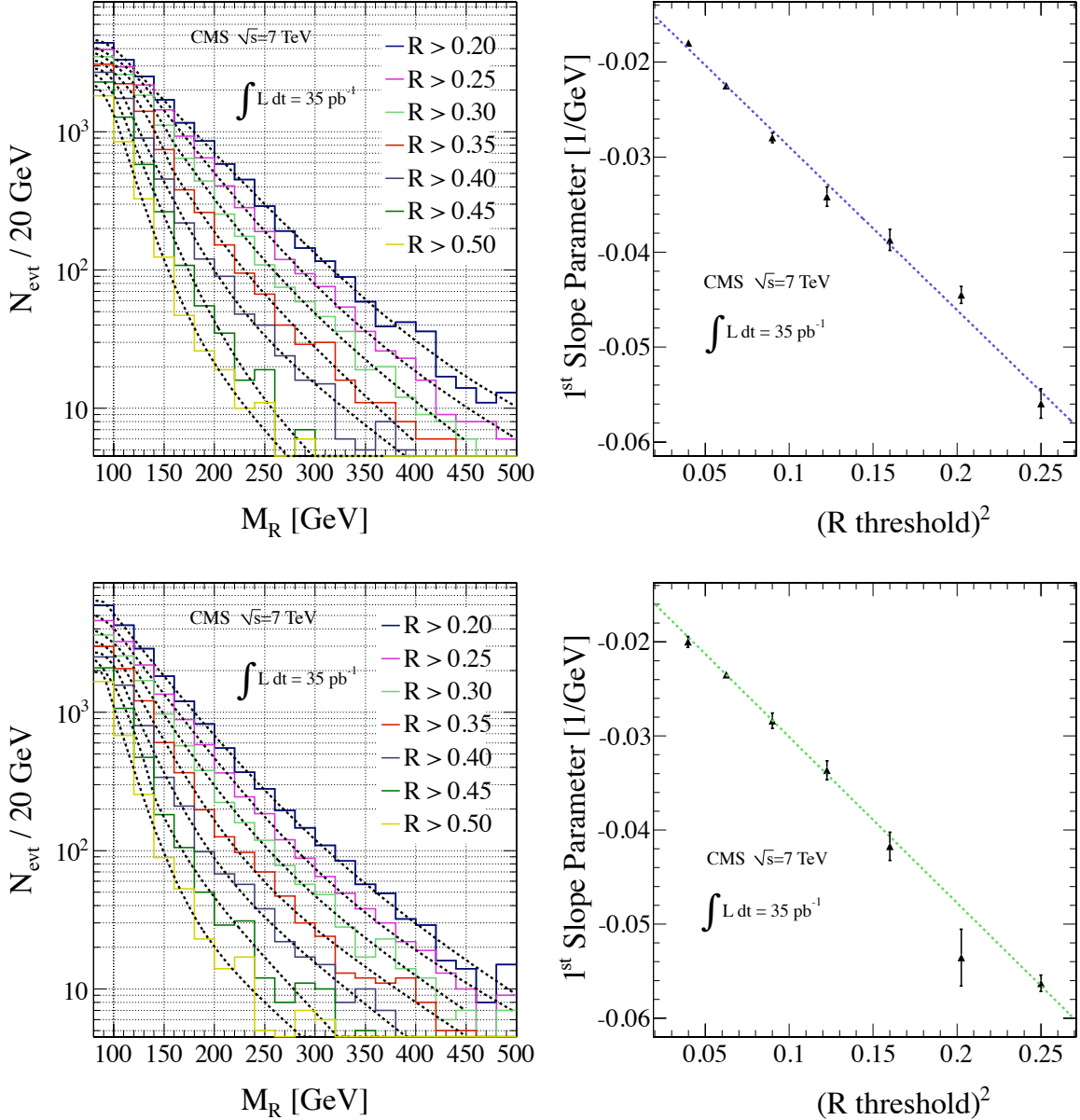


Figure 3: (Left) M_R distributions for different values of the R threshold from data events selected in the MU (upper) and ELE (lower) boxes. Dotted curves show the results of fits using two independent exponential functions and an asymmetric Gaussian at low M_R . (Right) The slope S of the first exponential component as a function of the square of the R threshold in the MU (upper) and ELE (lower) boxes. The dotted lines show the results of the fits to the form $S = a + bR^2$.

For the final background prediction the magnitude of the relative normalization between the two $W(\ell\nu)$ +jets components, denoted f^W , is determined from a binned maximum likelihood fit in the region $200 < M_R < 400$ GeV.

6 Results

6.1 Lepton box background predictions

Having extracted the M_R shape of the W +jets and Z +jets backgrounds, their relative normalization is set from the W and Z cross sections measured by CMS in electron and muon final states [30]. Similarly, the normalization of the $c\bar{c}$ background relative to W +jets is taken from the $t\bar{t}$ cross section measured by CMS in the dilepton channel [37]. The measured values of these cross sections are summarized below:

$$\begin{aligned} \sigma(pp \rightarrow WX) \times B(W \rightarrow \ell\nu) &= 9.951 \pm 0.073 \text{ (stat)} \pm 0.280 \text{ (syst)} \pm 1.095 \text{ (lum) nb ,} \\ \sigma(pp \rightarrow ZX) \times B(Z \rightarrow \ell\ell) &= 0.931 \pm 0.026 \text{ (stat)} \pm 0.023 \text{ (syst)} \pm 0.102 \text{ (lum) nb ,} \\ \sigma(pp \rightarrow t\bar{t}) &= 194 \pm 72 \text{ (stat)} \pm 24 \text{ (syst)} \pm 21 \text{ (lum) pb .} \end{aligned} \quad (10)$$

For an $R > 0.45$ threshold the QCD background is virtually eliminated. The region $125 < M_R < 175$ GeV where the QCD contribution is negligible and the $W(\ell\nu)$ +jets component is dominant is used to fix the overall normalization of the total background prediction. The final background prediction in the ELE and MU boxes for $R > 0.45$ is shown in Fig. 4.

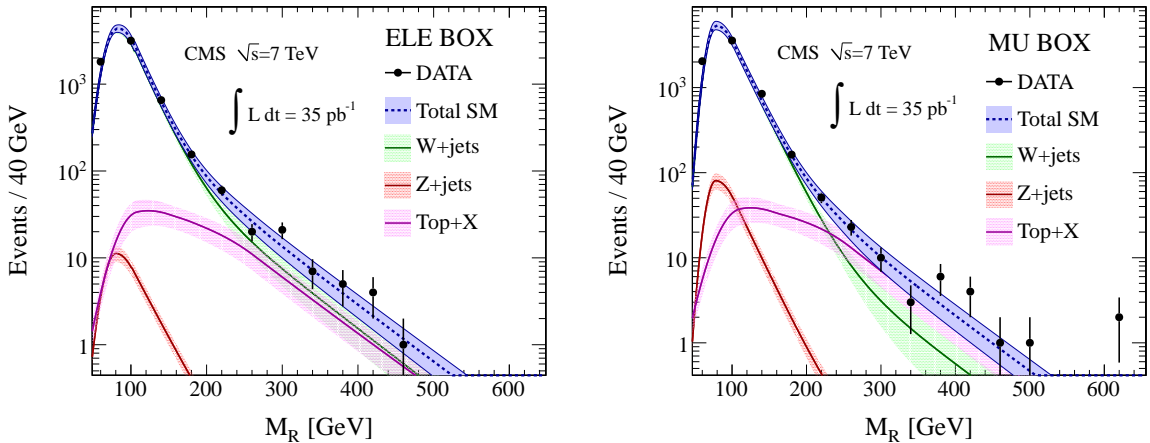


Figure 4: The M_R distributions with $R > 0.45$ in the ELE (left) and MU (right) boxes for data (points) and backgrounds (curves). The bands show the uncertainties of the background predictions.

The number of events with $M_R > 500$ GeV observed in data and the corresponding number of predicted background events are given in Table 1 for the ELE and MU boxes. Agreement between the predicted and observed yields is found. The p -value of the measurement in the MU box is 0.1, given the predicted background (with its statistical and systematic uncertainties) and the observed number of events. A summary of the uncertainties entering the background measurements is presented in Table 2.

Table 1: The number of predicted background events in the ELE and MU boxes for $R > 0.45$ and $M_R > 500 \text{ GeV}$ and the number of events observed in data.

	Predicted	Observed
ELE box	0.63 ± 0.23	0
MU box	0.51 ± 0.20	3

Table 2: Summary of the uncertainties on the background predictions for the ELE and MU boxes and their relative magnitudes. The range in the Monte Carlo uncertainties is owing to the different statistical precisions of the simulated background samples.

Parameter	Description	Relative magnitude
Slope parameter a	systematic bias from correlations in fits	5%
Slope parameter b	systematic bias from correlations in fits	10%
Slope parameter a	uncertainty from Monte Carlo	1–10%
Slope parameter b	uncertainty from Monte Carlo	1–10%
$\rho(a)^{\text{data/MC}}$	data fit	3%
$\rho(b)^{\text{data/MC}}$	data fit	3%
Normalization	systematic+statistical component	3–8%
f^W	extracted from fit (W only)	30%
$PW/\bar{t}t$ cross section ratio	CMS measurements (top only)	40%
W/Z cross section ratio	CMS measurements (Z only)	19%

6.2 Hadronic box background predictions

The procedure for estimating the total background predictions in the hadronic box is summarized as follows:

- Construct the non-QCD background shapes in M_R using measured values of a and b from simulated events, applying correction factors derived from data control samples, and taking into account the H_T trigger turn-on efficiency.
- Set the relative normalizations of the W+jets, Z+jets, and t+X backgrounds using the relevant inclusive cross section measurements from CMS (Eq. 10).
- Set the overall normalization by measuring the event yields in the lepton boxes, corrected for lepton reconstruction and identification efficiencies. The shapes and normalizations of all the non-QCD backgrounds are now fixed.
- The shape of the QCD background is extracted, as described in Section 5.1, and its normalization in the HAD box is determined from a fit to the low- M_R region, as described below.

The final hadronic box background prediction is calculated from a binned likelihood fit of the total background shape to the data in the interval $80 < M_R < 400 \text{ GeV}$ with all background normalizations and shapes fixed, except for the following free parameters: i) the H_T trigger turn-on shapes, ii) f^W as introduced in Section 5.2, and iii) the overall normalization of the QCD background. A set of pseudo-experiments is used to test the overall fit for coverage of the various floated parameters and for systematic biases. A 2% systematic uncertainty is assigned to the high- M_R background prediction that encapsulates systematic effects related to the fitting procedure. Figure 5 shows the final hadronic box background predictions with all uncertainties on this prediction included for $R > 0.5$. The observed M_R distribution is consistent with the predicted one over the entire M_R range. The predicted and observed background yields in the

high- M_R region are summarized in Table 3. A summary of the uncertainties entering these background predictions is listed in Table 4. A larger R requirement is used in the HAD box analysis due to the larger background.

Table 3: Predicted and observed yields for $M_R > 500 \text{ GeV}$ with $R > 0.5$ in the HAD box.

M_R	Predicted	Observed
$M_R > 500 \text{ GeV}$	5.5 ± 1.4	7

Table 4: Summary of uncertainties entering the background predictions for the HAD box.

Parameter	Description	Relative magnitude
Slope parameter a	systematic bias from correlations in fits	5%
Slope parameter b	systematic bias from correlations in fits	10%
Slope parameter a	uncertainty from Monte Carlo	1–10%
Slope parameter b	uncertainty from Monte Carlo	1–10%
$\rho(a)^{\text{data/MC}}$	data fit	3%
$\rho(b)^{\text{data/MC}}$	data fit	3%
Normalization	systematic+statistical component	8%
Trigger parameters	systematic from fit pseudo-experiments	2%
f^W	extracted from fit (W only)	13%
$W/t\bar{t}$ cross section ratio	CMS measurements (top only)	40%
W/Z cross section ratio	CMS measurements (Z only)	19%

7 Limits in the CMSSM Parameter Space

Having observed no significant excess of events beyond the SM expectations, we extract a model-independent 95% confidence level (CL) limit on the number of signal events. This limit is then interpreted in the parameter spaces of SUSY models.

The likelihood for the number of observed events n is modeled as a Poisson function, given the sum of the number of signal events (s) and the number of background events. A posterior probability density function $P(s)$ for the signal yield is derived using Bayes theorem, assuming a flat prior for the signal and a log-normal prior for the background.

The model-independent upper limit is derived by integrating the posterior probability density function between 0 and s^* so that $\int_0^{s^*} P(s)ds = 0.95$. The observed upper limit in the hadronic box is $s^* = 8.4$ (expected limit 7.2 ± 2.7); in the muon box $s^* = 6.3$ (expected limit 3.5 ± 1.1); and in the electron box $s^* = 2.9$ (expected limit 3.6 ± 1.1). For 10% of the pseudo-experiments in the muon box the expected limit is higher than the observed. The stability of the result was studied with different choices of the signal prior. In particular, using the reference priors derived with the methods described in Ref. [38], the observed upper limits in the hadronic, muon, and electron boxes are 8.0, 5.3, and 2.9, respectively.

The results can be interpreted in the context of the CMSSM, which is a truncation of the full SUSY parameter space motivated by the minimal supergravity framework for spontaneous soft breaking of supersymmetry. In the CMSSM the soft breaking parameters are reduced to five: three mass parameters m_0 , $m_{1/2}$, and A_0 being, respectively, a universal scalar mass, a universal gaugino mass, and a universal trilinear scalar coupling, as well as $\tan \beta$, the ratio of the up-type and down-type Higgs vacuum expectation values, and the sign of the supersymmetric

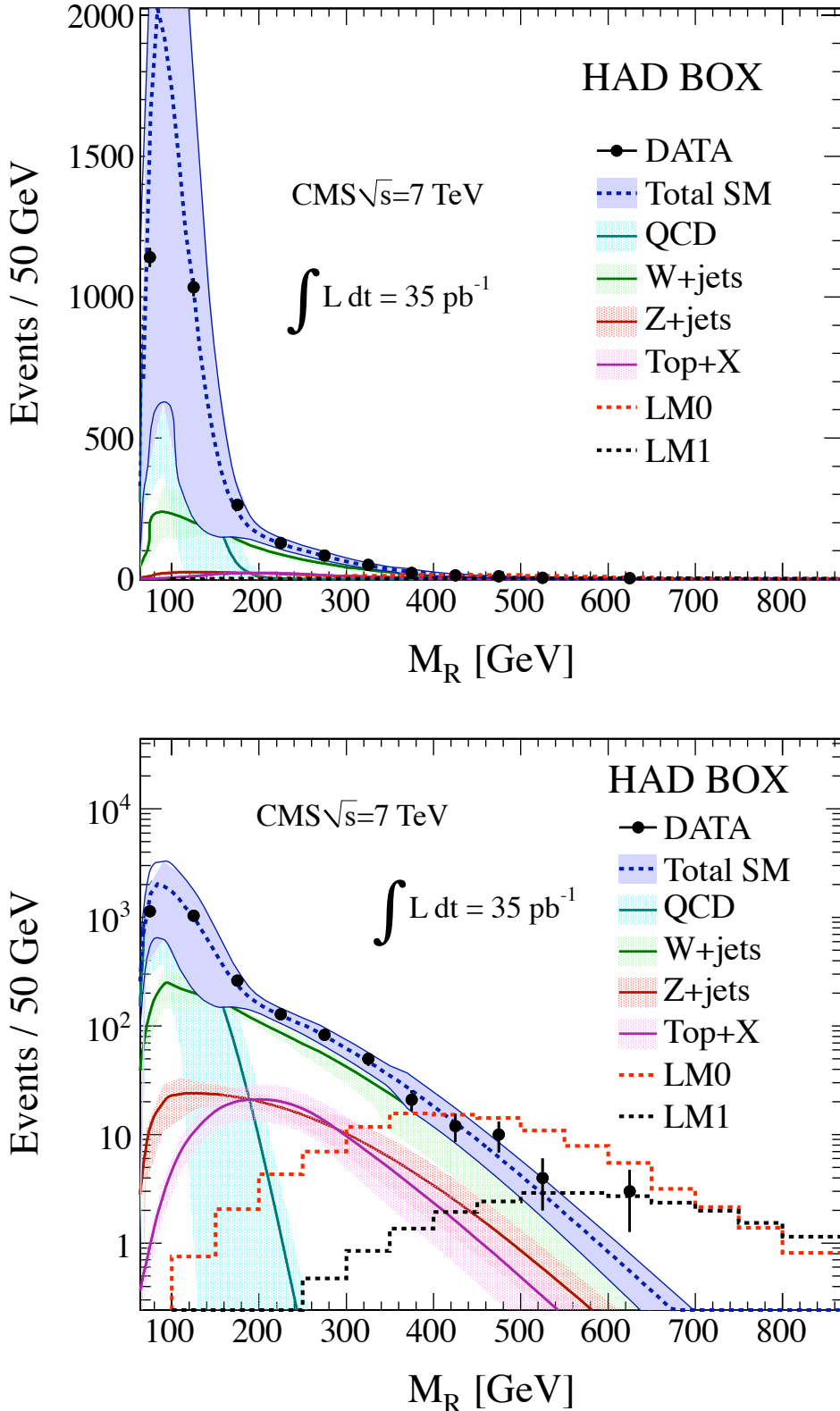


Figure 5: The M_R distributions with $R > 0.5$ in the HAD box for data (points) and backgrounds (curves) on (top) linear and (bottom) logarithmic scales. The bands show the uncertainties of the background predictions. The corresponding distributions for SUSY benchmark models LM1 [18] with $M_\Delta = 597 \text{ GeV}$ and LM0 [14] with $M_\Delta = 400 \text{ GeV}$ are overlaid.

Higgs mass parameter μ . Scanning over these parameters yields models which, while not entirely representative of the complete SUSY parameter space, vary widely in their superpartner spectra and thus in the dominant production channels and decay chains.

The upper limits are projected onto the $(m_0, m_{1/2})$ plane by comparing them with the predicted yields, and excluding any model if $s(m_0, m_{1/2}) > s^*$. The systematic uncertainty on the signal yield (coming from the uncertainty on the luminosity, the selection efficiency, and the theoretical uncertainty associated with the cross section calculation) is modeled according to a log-normal prior. The uncertainty on the selection efficiency includes the effect of jet energy scale (JES) corrections, parton distribution function (PDF) uncertainties [39], and the description of initial-state radiation (ISR). All the effects are summed in quadrature as shown in Table 5. The JES, ISR, and PDF uncertainties are relatively small owing to the insensitivity of the signal R and M_R distributions to these effects.

Table 5: Summary of the systematic uncertainties on the signal yield and totals for each of the event boxes. For the CMSSM scan the NLO signal cross section uncertainty is included.

box	MU	ELE	HAD
Experiment			
JES	1%	1%	1%
Data/MC ϵ	6%	6%	6%
\mathcal{L} [40]	4%	4%	4%
Theory			
ISR	1%	1%	0.5%
PDF	3–6%	3–6%	3–6%
Subtotal	8–9%	8–9%	8–9%
CMSSM			
NLO	16–18%	16–18%	16–18%
Total	17–19%	17–19%	17–19%

The observed limits from the ELE, MU, and HAD boxes are shown in Figs. 6, 7, and 8, respectively, in the CMSSM $(m_0, m_{1/2})$ plane for the values $\tan\beta = 3$, $A_0 = 0$, $\text{sgn}(\mu) = +1$, together with the 68% probability band for the expected limits, obtained by applying the same procedure to an ensemble of background-only pseudo-experiments. The band is computed around the median of the limit distribution. Observed limits are also shown in Figs. 9–11 in the CMSSM $(m_0, m_{1/2})$ plane for the values $\tan\beta = 10$, $A_0 = 0$, $\text{sgn}(\mu) = +1$, and in Figs. 12–13 for the values $\tan\beta = 50$, $A_0 = 0$, $\text{sgn}(\mu) = +1$.

Figure 14 shows the same result in terms of 95% CL upper limits on the cross section as a function of the physical masses for two benchmark simplified models [13, 41–43]: four-flavor squark pair production and gluino pair production. In the former, each squark decays to one quark and the LSP, resulting in final states with two jets and missing transverse energy, while in the latter each gluino decays directly to two light quarks and the LSP, giving events with four jets and missing transverse energy.

8 Summary

We performed a search for squarks and gluinos using a data sample of 35 pb^{-1} integrated luminosity from pp collisions at $\sqrt{s} = 7 \text{ TeV}$, recorded by the CMS detector at the LHC. The kinematic consistency of the selected events was tested against the hypothesis of heavy particle

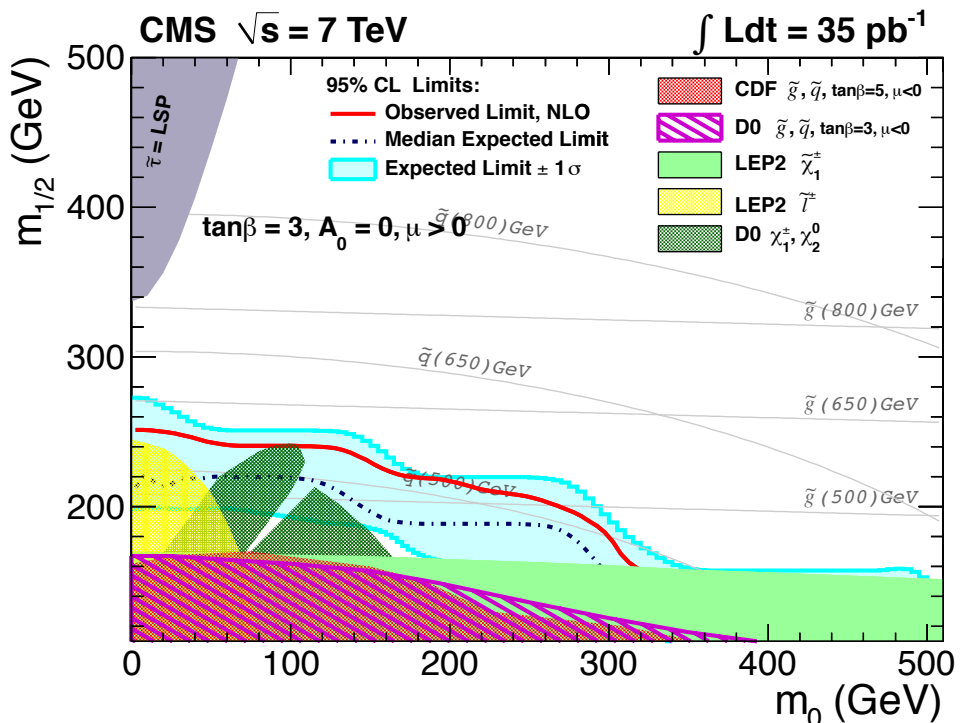


Figure 6: Observed (solid curve) and expected (dot-dashed curve) 95% CL limits in the $(m_0, m_{1/2})$ CMSSM plane with $\tan\beta = 3$, $A_0 = 0$, $\text{sgn}(\mu) = +1$ from the ELE box selection ($R > 0.45$, $M_R > 500 \text{ GeV}$). The ± 1 standard deviation equivalent variations in the uncertainties are shown as a band around the expected limits. The area labeled $\tilde{\tau} = \text{LSP}$ is the region of the parameter space where the LSP is a $\tilde{\tau}$ and not the lightest neutralino.

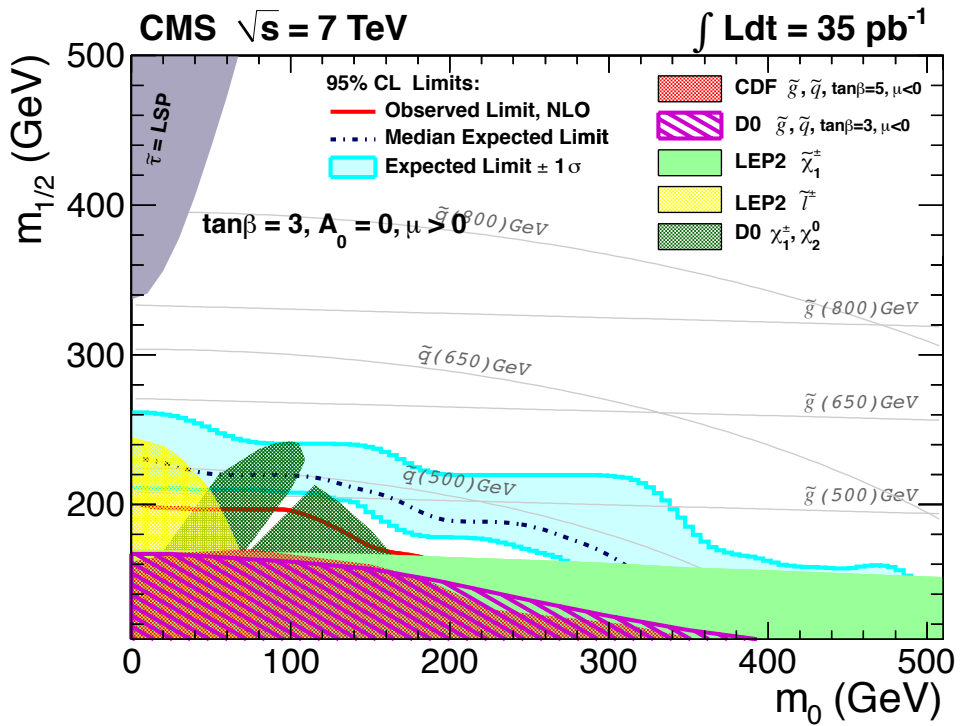


Figure 7: Observed (solid curve) and expected (dot-dashed curve) 95% CL limits in the $(m_0, m_{1/2})$ CMSSM plane with $\tan \beta = 3$, $A_0 = 0$, $\text{sgn}(\mu) = +1$ from the MU box selection ($R > 0.45$, $M_R > 500 \text{ GeV}$). The \pm one standard deviation equivalent variations in the uncertainties are shown as a band around the expected limits.

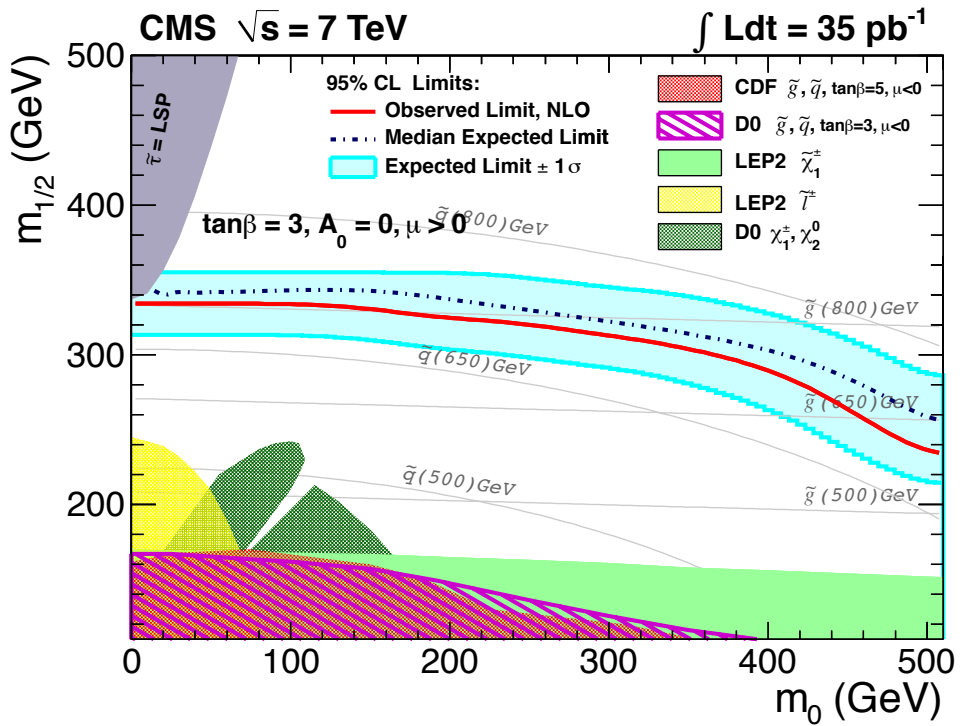


Figure 8: Observed (solid curve) and expected (dot-dashed curve) 95% CL limits in the $(m_0, m_{1/2})$ CMSSM plane with $\tan\beta = 3, A_0 = 0, \text{sgn}(\mu) = +1$ from the HAD box selection ($R > 0.5, M_R > 500 \text{ GeV}$). The ± 1 standard deviation equivalent variations in the uncertainties are shown as a band around the expected limits.

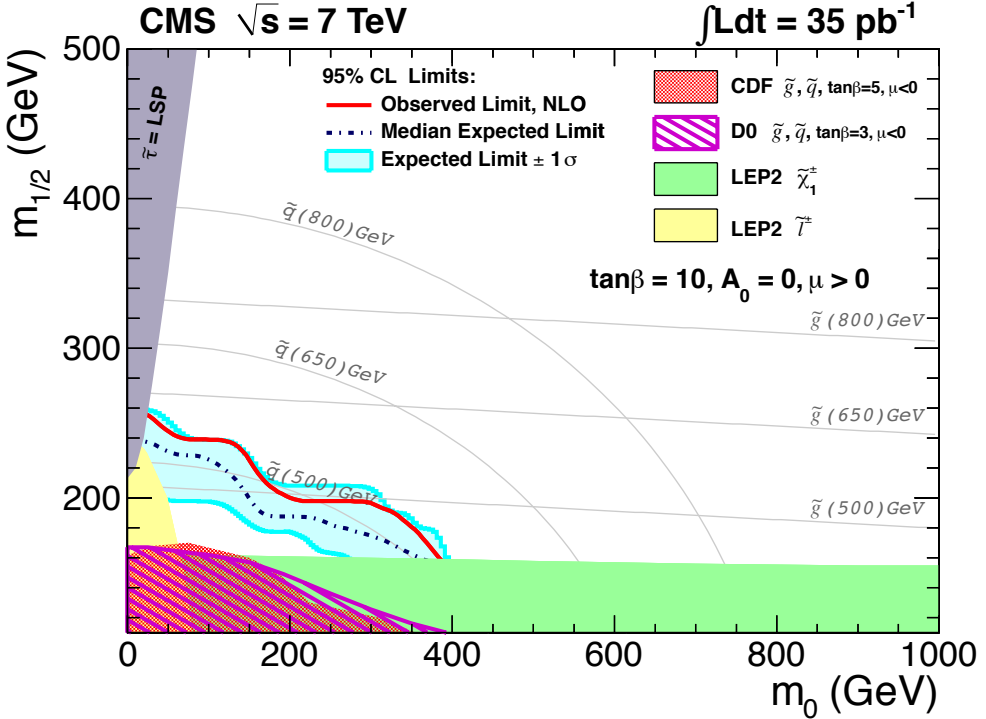


Figure 9: Observed (solid curve) and expected (dot-dashed curve) 95% CL limits in the $(m_0, m_{1/2})$ CMSSM plane with $\tan\beta = 10$, $A_0 = 0$, $\text{sgn}(\mu) = +1$ from the ELE box selection ($R > 0.45$, $M_R > 500 \text{ GeV}$). The \pm one standard deviation equivalent variations in the uncertainties are shown as a band around the expected limits.

pair production using the dimensionless razor variable R related to the missing transverse energy E_T^{miss} , and M_R , an event-by-event indicator of the heavy particle mass scale. We used events with large R and high M_R in inclusive topologies.

The search relied on predictions of the SM backgrounds determined from data samples dominated by SM processes. No significant excess over the background expectations was observed, and model-independent upper limits on the numbers of signal events were calculated. The results were presented in the $(m_0, m_{1/2})$ CMSSM parameter space. For simplified models the results were given as limits on the production cross sections as a function of the squark, gluino, and LSP masses.

These results demonstrate the strengths of the razor analysis approach; the simple exponential behavior of the various SM backgrounds when described in terms of the razor variables is useful in suppressing these backgrounds and in making reliable estimates from data of the background residuals in the signal regions. Hence, the razor method provides an additional powerful probe in searching for physics beyond the SM at the LHC.

Acknowledgments

We wish to congratulate our colleagues in the CERN accelerator departments for the excellent performance of the LHC machine. We thank the technical and administrative staff at CERN and other CMS institutes. This work was supported by the Austrian Federal Ministry of Science and Research; the Belgian Fonds de la Recherche Scientifique, and Fonds voor Wetenschap-

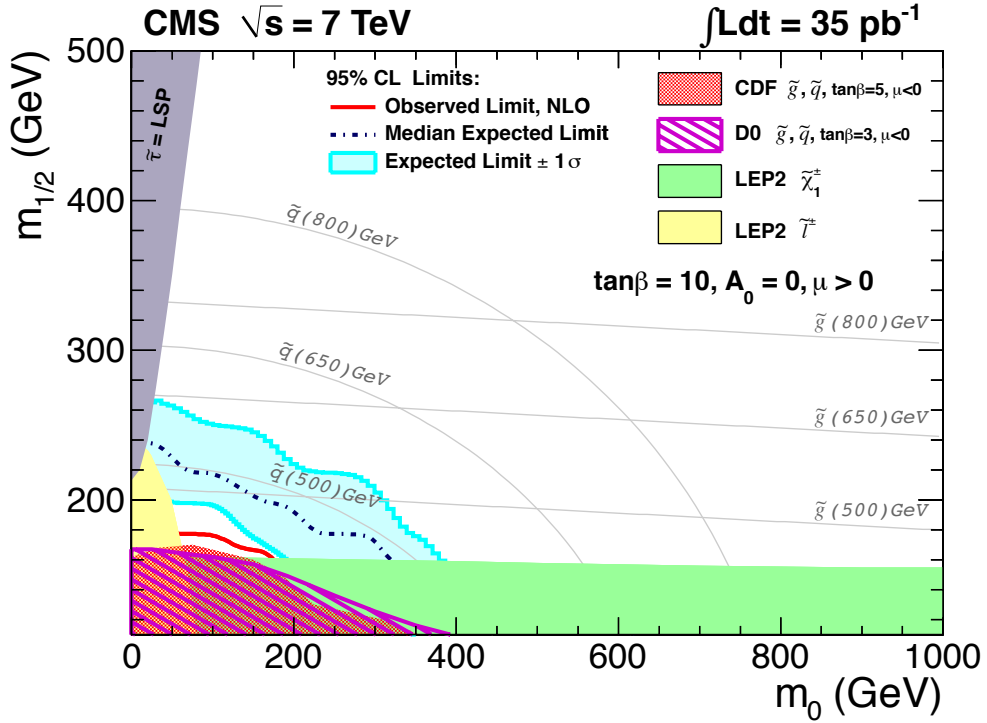


Figure 10: Observed (solid curve) and expected (dot-dashed curve) 95% CL limits in the $(m_0, m_{1/2})$ CMSSM plane with $\tan\beta = 10$, $A_0 = 0$, $\text{sgn}(\mu) = +1$ from the MU box selection ($R > 0.45$, $M_R > 500 \text{ GeV}$). The \pm one standard deviation equivalent variations in the uncertainties are shown as a band around the expected limits.

pelijk Onderzoek; the Brazilian Funding Agencies (CNPq, CAPES, FAPERJ, and FAPESP); the Bulgarian Ministry of Education and Science; CERN; the Chinese Academy of Sciences, Ministry of Science and Technology, and National Natural Science Foundation of China; the Colombian Funding Agency (COLCIENCIAS); the Croatian Ministry of Science, Education and Sport; the Research Promotion Foundation, Cyprus; the Estonian Academy of Sciences and NICPB; the Academy of Finland, Finnish Ministry of Education and Culture, and Helsinki Institute of Physics; the Institut National de Physique Nucléaire et de Physique des Particules / CNRS, and Commissariat à l’Énergie Atomique et aux Énergies Alternatives / CEA, France; the Bundesministerium für Bildung und Forschung, Deutsche Forschungsgemeinschaft, and Helmholtz-Gemeinschaft Deutscher Forschungszentren, Germany; the General Secretariat for Research and Technology, Greece; the National Scientific Research Foundation, and National Office for Research and Technology, Hungary; the Department of Atomic Energy and the Department of Science and Technology, India; the Institute for Studies in Theoretical Physics and Mathematics, Iran; the Science Foundation, Ireland; the Istituto Nazionale di Fisica Nucleare, Italy; the Korean Ministry of Education, Science and Technology and the World Class University program of NRF, Korea; the Lithuanian Academy of Sciences; the Mexican Funding Agencies (CINVESTAV, CONACYT, SEP, and UASLP-FAI); the Ministry of Science and Innovation, New Zealand; the Pakistan Atomic Energy Commission; the State Commission for Scientific Research, Poland; the Fundação para a Ciência e a Tecnologia, Portugal; JINR (Armenia, Belarus, Georgia, Ukraine, Uzbekistan); the Ministry of Science and Technologies of the Russian Federation, and Russian Ministry of Atomic Energy; the Ministry of Science and Technological Development of Serbia; the Ministerio de Ciencia e Innovación, and Programa Consolider-Ingenio 2010, Spain; the Swiss Funding Agencies (ETH Board, ETH Zurich, PSI, SNF, UniZH,

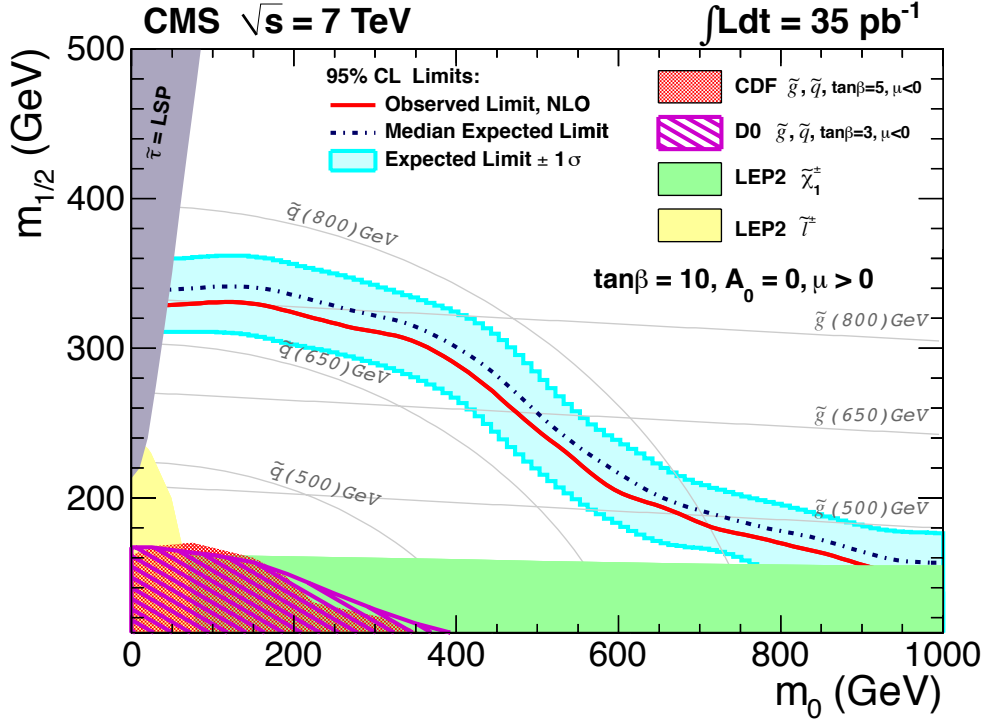


Figure 11: Observed (solid curve) and expected (dot-dashed curve) 95% CL limits in the $(m_0, m_{1/2})$ CMSSM plane with $\tan\beta = 10$, $A_0 = 0$, $\text{sgn}(\mu) = +1$ from the HAD box selection ($R > 0.5$, $M_R > 500 \text{ GeV}$). The ± 1 standard deviation equivalent variations in the uncertainties are shown as a band around the expected limits.

Canton Zurich, and SER); the National Science Council, Taipei; the Scientific and Technical Research Council of Turkey, and Turkish Atomic Energy Authority; the Science and Technology Facilities Council, UK; the US Department of Energy, and the US National Science Foundation.

Individuals have received support from the Marie-Curie programme and the European Research Council (European Union); the Leventis Foundation; the A. P. Sloan Foundation; the Alexander von Humboldt Foundation; the Associazione per lo Sviluppo Scientifico e Tecnologico del Piemonte (Italy); the Belgian Federal Science Policy Office; the Fonds pour la Formation à la Recherche dans l’Industrie et dans l’Agriculture (FRIA-Belgium); the Agentschap voor Innovatie door Wetenschap en Technologie (IWT-Belgium); and the Council of Science and Industrial Research, India.

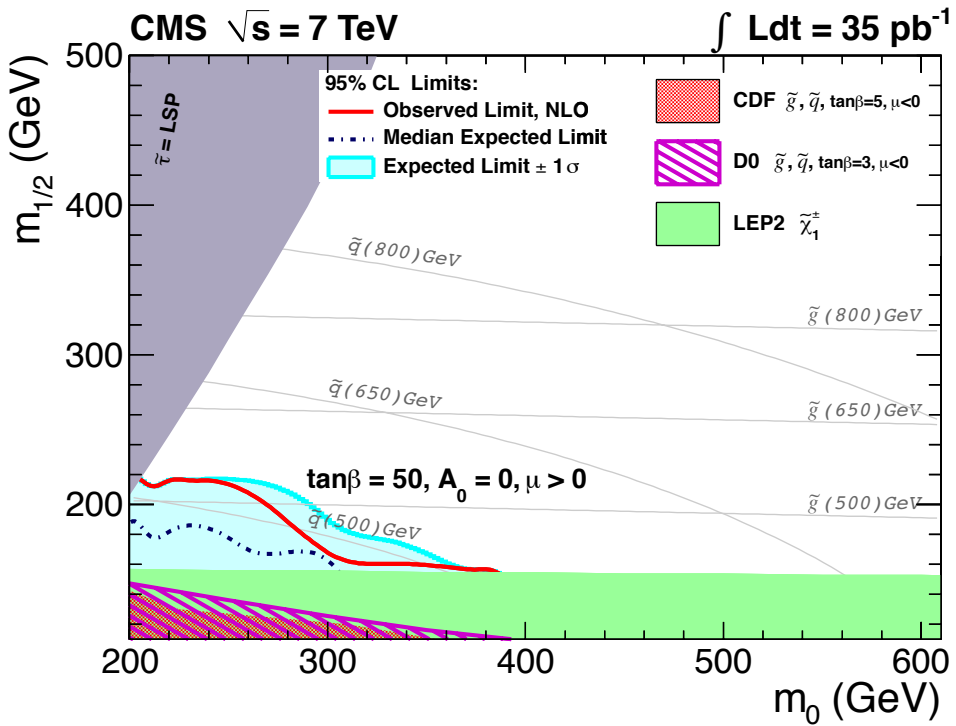


Figure 12: Observed (solid curve) and expected (dot-dashed curve) 95% CL limits in the $(m_0, m_{1/2})$ CMSSM plane with $\tan\beta = 50$, $A_0 = 0$, $\text{sgn}(\mu) = +1$ from the ELE box selection ($R > 0.45$, $M_R > 500 \text{ GeV}$). The ± 1 standard deviation equivalent variations in the uncertainties are shown as a band around the expected limits.

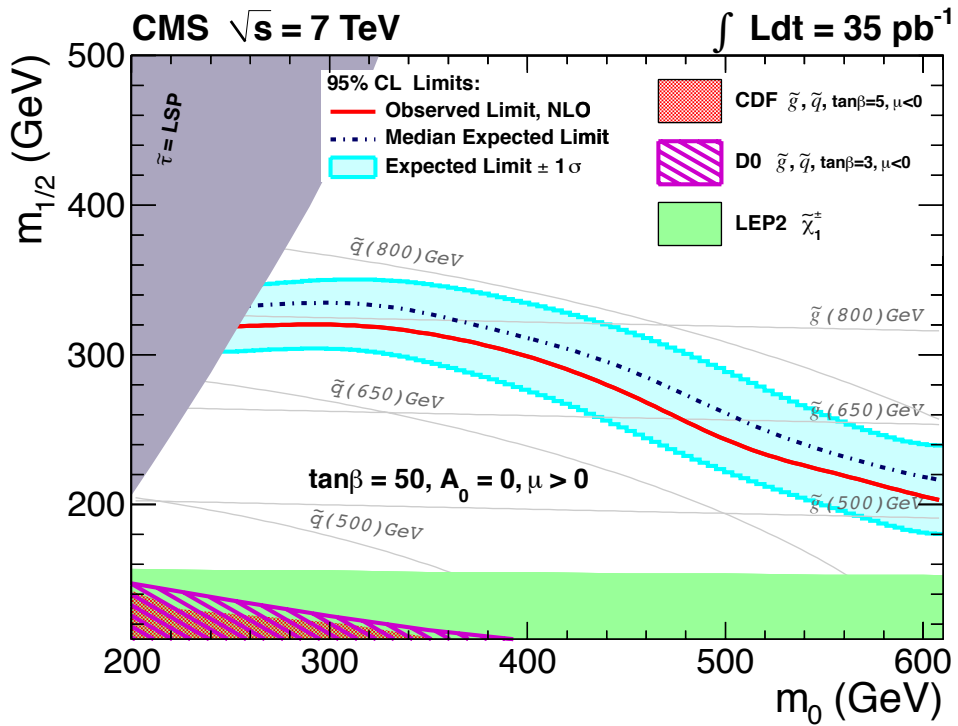


Figure 13: Observed (solid curve) and expected (dot-dashed curve) 95% L limits in the $(m_0, m_{1/2})$ CMSSM plane with $\tan\beta = 50$, $A_0 = 0$, $\text{sgn}(\mu) = +1$ from the HAD box selection ($R > 0.5$, $M_R > 500 \text{ GeV}$). The ± 1 standard deviation equivalent variations in the uncertainties are shown as a band around the expected limits.

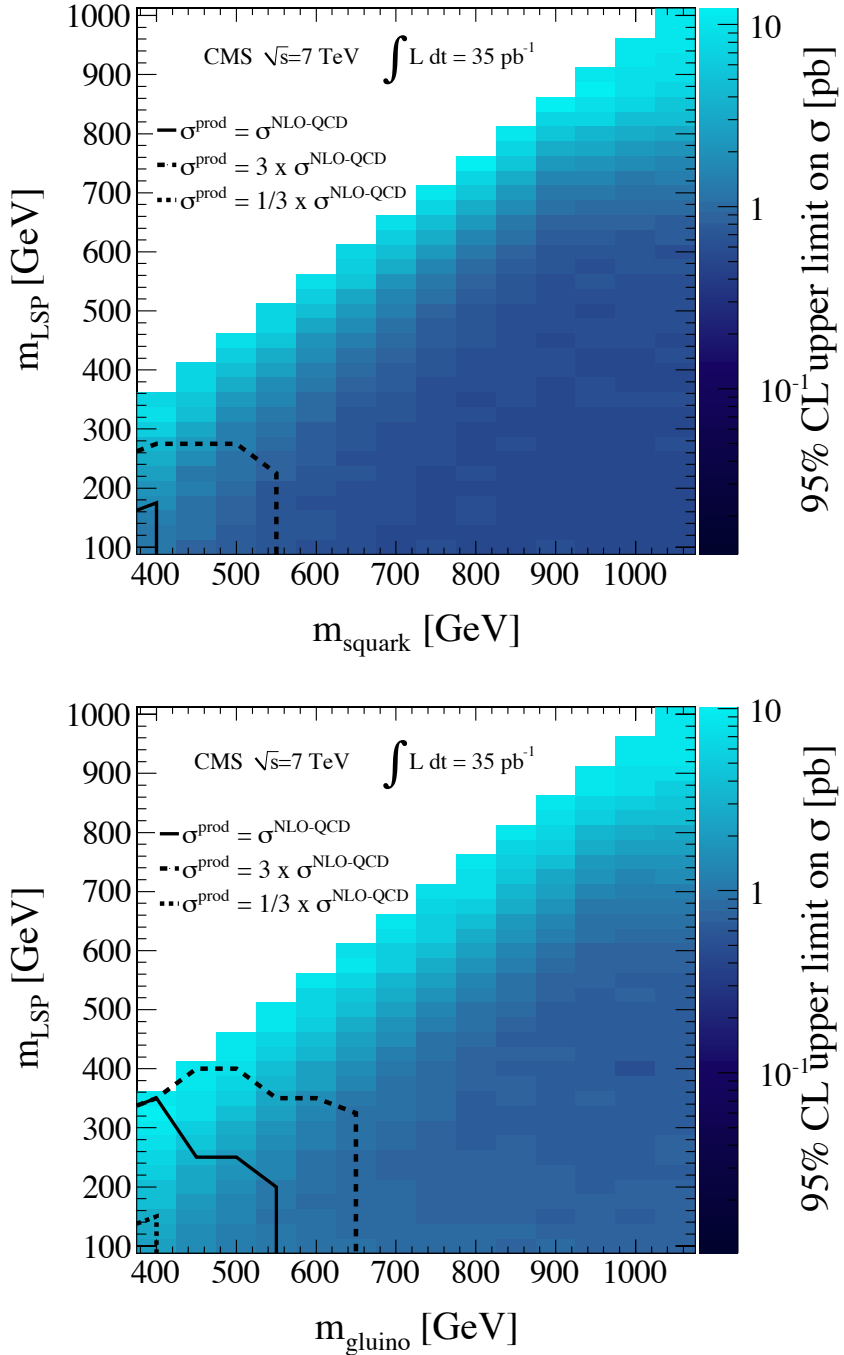


Figure 14: Upper limits on two simplified models: di-squark production (top) resulting in a 2-jet + E_T^{miss} final state and di-gluino (lower) production resulting in a 4-jet + E_T^{miss} final state. The shade scale indicates the value of the cross section excluded at 95% CL for each value of m_{LSP} and m_{gluino} or m_{squark} . The solid and dashed contours indicate the 95% CL limits assuming the NLO cross section and its variations up and down by a factor of three.

References

- [1] P. Ramond, "Dual Theory for Free Fermions", *Phys. Rev. D* **3** (1971) 2415.
`doi:10.1103/PhysRevD.3.2415.`
- [2] Y. Golfand and E. Likhtman, "Extension of the Algebra of Poincare Group Generators and Violation of p Invariance", *JETP Lett.* **13** (1971) 323.
- [3] D. Volkov and V. Akulov, "Possible universal neutrino interaction", *JETP Lett.* **16** (1972) 438.
- [4] J. Wess and B. Zumino, "Supergauge Transformations in Four-Dimensions", *Nucl. Phys. B* **70** (1974) 39. `doi:10.1016/0550-3213(74)90355-1.`
- [5] P. Fayet, "Supergauge Invariant Extension of the Higgs Mechanism and a Model for the Electron and Its Neutrino", *Nucl. Phys. B* **90** (1975) 104.
`doi:10.1016/0550-3213(75)90636-7.`
- [6] C. Rogan, "Kinematics for new dynamics at the LHC", (2010). `arXiv:1006.2727.`
`CALT-68-2790.`
- [7] D0 Collaboration, "Search for squarks and gluinos in events with jets and missing transverse energy using 2.1 fb^{-1} of $p\bar{p}$ collision data at $\sqrt{s} = 1.96 \text{ TeV}$ ", *Phys. Lett. B* **660** (2008) 449, `arXiv:0712.3805.` `doi:10.1016/j.physletb.2008.01.042.`
- [8] CDF Collaboration, "Inclusive Search for Squark and Gluino Production in p anti-p Collisions at $\sqrt{s} = 1.96 \text{ TeV}$ ", *Phys. Rev. Lett.* **102** (2009) 121801, `arXiv:0811.2512.`
`doi:10.1103/PhysRevLett.102.121801.`
- [9] ATLAS Collaboration, "Search for an excess of events with an identical flavour lepton pair and significant missing transverse momentum in $\sqrt{s} = 7 \text{ TeV}$ proton-proton collisions with the ATLAS detector", (2011). `arXiv:1103.6208.` Accepted by EPJC.
- [10] ATLAS Collaboration, "Search for squarks and gluinos using final states with jets and missing transverse momentum with the ATLAS detector in $\sqrt{s} = 7 \text{ TeV}$ proton-proton collisions", *Phys. Lett. B* **701** (2011) 186, `arXiv:1102.5290.`
`doi:10.1016/j.physletb.2011.05.061.`
- [11] ATLAS Collaboration, "Search for supersymmetry using final states with one lepton, jets, and missing transverse momentum with the ATLAS detector in $\sqrt{s} = 7 \text{ TeV}$ pp collisions", *Phys. Rev. Lett.* **106** (2011) 131802, `arXiv:1102.2357.`
`doi:10.1103/PhysRevLett.106.131802.`
- [12] ATLAS Collaboration, "Search for supersymmetric particles in events with lepton pairs and large missing transverse momentum in $\sqrt{s} = 7 \text{ TeV}$ proton-proton collisions with the ATLAS experiment", (2011). `arXiv:1103.6214.` Accepted by EPJC.
- [13] CMS Collaboration, "Search for new physics at CMS with jets and missing momentum", *CMS Physics Analysis Summary CMS-PAS-SUS-10-005* (2010).
- [14] CMS Collaboration, "Search for Supersymmetry in pp Collisions at 7 TeV in Events with Jets and Missing Transverse Energy", *Phys. Lett. B* **698** (2011) 196, `arXiv:1101.1628.`
`doi:10.1016/j.physletb.2011.03.021.`

- [15] CMS Collaboration, “Search for new physics with same-sign isolated dilepton events with jets and missing transverse energy at the LHC”, *Journal of High Energy Physics* **2011** (2011) 1, arXiv:1104.3168. doi:10.1007/JHEP06(2011)077.
- [16] CMS Collaboration, “Search for Physics Beyond the Standard Model in Opposite-Sign Dilepton Events at $\sqrt{s} = 7$ TeV”, (2011). arXiv:1103.1348. CMS-SUS-10-007, CERN-EP-PH-2011-016.
- [17] CMS Collaboration, “The CMS experiment at the CERN LHC”, *JINST* **3** (2008) S08004. doi:10.1088/1748-0221/3/08/S08004.
- [18] CMS Collaboration, “CMS technical design report, volume II: Physics performance”, *J. Phys. G* **34** (2007) 995. doi:10.1088/0954-3899/34/6/S01.
- [19] T. Sjöstrand, S. Mrenna, and P. Skands, “PYTHIA 6.4 Physics and Manual; v6.420, tune D6T”, *JHEP* **05** (2006) 026, arXiv:hep-ph/0603175.
- [20] F. Maltoni and T. Stelzer, “MadEvent: Automatic event generation with MadGraph”, *JHEP* **02** (2003) 027, arXiv:hep-ph/0208156.
- [21] GEANT4 Collaboration, “GEANT4: A simulation toolkit”, *Nucl. Instrum. Meth. A* **506** (2003) 250. doi:10.1016/S0168-9002(03)01368-8.
- [22] B. C. Allanach, “SOFTSUSY: a program for calculating supersymmetric spectra”, *Comput. Phys. Commun.* **143** (2002) 305, arXiv:hep-ph/0104145. doi:10.1016/S0010-4655(01)00460-X.
- [23] A. Djouadi, M. M. Muhlleitner, and M. Spira, “Decays of Supersymmetric Particles: the program SUSY-HIT (SUspect-SdecaY-Hdecay-InTerface)”, *Acta Phys. Polon. B* **38** (2007) 635, arXiv:hep-ph/0609292.
- [24] P. Z. Skands et al., “SUSY Les Houches Accord: Interfacing SUSY Spectrum Calculators, Decay Packages, and Event Generators”, *JHEP* **07** (2004) 036, arXiv:hep-ph/0311123. doi:10.1088/1126-6708/2004/07/036.
- [25] W. Beenakker, R. Hopker, and M. Spira, “PROSPINO: A program for the Production of Supersymmetric Particles in Next-to-leading Order QCD”, (1996). arXiv:hep-ph/9611232.
- [26] CMS Collaboration, “Tracking and Primary Vertex Results in First 7 TeV Collisions”, *CMS Physics Analysis Summary* **CMS-PAS-TRK-10-005** (2010).
- [27] M. Cacciari, G. P. Salam, and G. Soyez, “The anti- k_t jet clustering algorithm”, *JHEP* **0804** (2008) 063. doi:10.1088/1126-6708/2008/04/063.
- [28] CMS Collaboration, “Determination of the Jet Energy Scale in CMS with pp Collisions at $\sqrt{s} = 7$ TeV”, *CMS Physics Analysis Summary* **CMS-PAS-JME-10-010** (2010).
- [29] CMS Collaboration, “Commissioning of the Particle-Flow Reconstruction in Minimum-Bias and Jet Events from pp Collisions at 7 TeV”, *CMS Physics Analysis Summary* **CMS-PAS-PFT-10-002** (2010).
- [30] CMS Collaboration, “Measurements of Inclusive W and Z Cross Sections in pp Collisions at $\sqrt{s} = 7$ TeV”, *CMS Physics Analysis Summary* **CMS-PAS-EWK-10-005** (2010).

-
- [31] A. H. Chamseddine, R. L. Arnowitt, and P. Nath, “Locally Supersymmetric Grand Unification”, *Phys. Rev. Lett.* **49** (1982) 970. doi:10.1103/PhysRevLett.49.970.
- [32] R. Barbieri, S. Ferrara, and C. A. Savoy, “Gauge Models with Spontaneously Broken Local Supersymmetry”, *Phys. Lett. B* **119** (1982) 343. doi:10.1016/0370-2693(82)90685-2.
- [33] L. J. Hall, J. D. Lykken, and S. Weinberg, “Supergravity as the Messenger of Supersymmetry Breaking”, *Phys. Rev. D* **27** (1983) 2359. doi:10.1103/PhysRevD.27.2359.
- [34] G. L. Kane, C. F. Kolda, L. Roszkowski et al., “Study of constrained minimal supersymmetry”, *Phys. Rev. D* **49** (1994) 6173, arXiv:hep-ph/9312272. doi:10.1103/PhysRevD.49.6173.
- [35] CMS Collaboration, “HCAL performance from first collisions data”, *CMS Detector Performance Summary* **DPS-2010-025** (2010).
- [36] CMS Collaboration, “Electromagnetic calorimeter commissioning and first results with 7 TeV data”, *CMS Note* **CMS-NOTE-2010-012** (2010).
- [37] CMS Collaboration, “First Measurement of the Cross Section for Top-Quark Pair Production in Proton-Proton Collisions at $\sqrt{s}=7$ TeV”, *Phys. Lett. B* **695** (2011) 424, arXiv:1010.5994. doi:10.1016/j.physletb.2010.11.058.
- [38] L. Demortier, S. Jain, and H. B. Prosper, “Reference priors for high energy physics”, *Phys. Rev. D* **82** (2010) 034002, arXiv:1002.1111. doi:10.1103/PhysRevD.82.034002.
- [39] D. Bourilkov, R. C. Group, and M. R. Whalley, “LHAPDF: PDF use from the Tevatron to the LHC”, (2006). arXiv:hep-ph/0605240.
- [40] CMS Collaboration, “Absolute luminosity normalization”, *CMS Detector Performance Summary* **CMS-DP-2011-002** (2011).
- [41] J. Alwall, P. Schuster, and N. Toro, “Simplified Models for a First Characterization of New Physics at the LHC”, *Phys. Rev. D* **79** (2009) 075020, arXiv:0810.3921. doi:10.1103/PhysRevD.79.075020.
- [42] J. Alwall, M. P. Le, M. Lisanti et al., “Searching for gluinos at the Tevatron and beyond”, *Int. J. Mod. Phys. A* **23** (2008) 4637. doi:10.1142/S0217751X0804281X.
- [43] D. Alves, N. Arkani-Hamed, S. Arora et al., “Simplified Models for LHC New Physics Searches”, (2011). arXiv:1105.2838.

A The CMS Collaboration

Yerevan Physics Institute, Yerevan, Armenia

S. Chatrchyan, V. Khachatryan, A.M. Sirunyan, A. Tumasyan

Institut für Hochenergiephysik der OeAW, Wien, Austria

W. Adam, T. Bergauer, M. Dragicevic, J. Erö, C. Fabjan, M. Friedl, R. Frühwirth, V.M. Ghete, J. Hammer¹, S. Hänsel, M. Hoch, N. Hörmann, J. Hrubec, M. Jeitler, W. Kiesenhofer, M. Krammer, D. Liko, I. Mikulec, M. Pernicka, B. Rahbaran, H. Rohringer, R. Schöfbeck, J. Strauss, A. Taurok, F. Teischinger, P. Wagner, W. Waltenberger, G. Walzel, E. Widl, C.-E. Wulz

National Centre for Particle and High Energy Physics, Minsk, Belarus

V. Mossolov, N. Shumeiko, J. Suarez Gonzalez

Universiteit Antwerpen, Antwerpen, Belgium

S. Bansal, L. Benucci, E.A. De Wolf, X. Janssen, T. Maes, L. Mucibello, S. Ochesanu, B. Roland, R. Rougny, M. Selvaggi, H. Van Haevermaet, P. Van Mechelen, N. Van Remortel

Vrije Universiteit Brussel, Brussel, Belgium

F. Blekman, S. Blyweert, J. D'Hondt, O. Devroede, R. Gonzalez Suarez, A. Kalogeropoulos, M. Maes, W. Van Doninck, P. Van Mulders, G.P. Van Onsem, I. Villella

Université Libre de Bruxelles, Bruxelles, Belgium

O. Charaf, B. Clerbaux, G. De Lentdecker, V. Dero, A.P.R. Gay, G.H. Hammad, T. Hreus, P.E. Marage, A. Raval, L. Thomas, C. Vander Velde, P. Vanlaer

Ghent University, Ghent, Belgium

V. Adler, A. Cimmino, S. Costantini, M. Grunewald, B. Klein, J. Lellouch, A. Marinov, J. Mccartin, D. Ryckbosch, F. Thyssen, M. Tytgat, L. Vanelderen, P. Verwilligen, S. Walsh, N. Zaganidis

Université Catholique de Louvain, Louvain-la-Neuve, Belgium

S. Basegmez, G. Bruno, J. Caudron, L. Ceard, E. Cortina Gil, J. De Favereau De Jeneret, C. Delaere, D. Favart, A. Giammacco, G. Grégoire, J. Hollar, V. Lemaitre, J. Liao, O. Militaru, C. Nuttens, S. Ovyn, D. Pagano, A. Pin, K. Piotrzkowski, N. Schul

Université de Mons, Mons, Belgium

N. Beliy, T. Caebergs, E. Daubie

Centro Brasileiro de Pesquisas Fisicas, Rio de Janeiro, Brazil

G.A. Alves, L. Brito, D. De Jesus Damiao, M.E. Pol, M.H.G. Souza

Universidade do Estado do Rio de Janeiro, Rio de Janeiro, Brazil

W.L. Aldá Júnior, W. Carvalho, E.M. Da Costa, C. De Oliveira Martins, S. Fonseca De Souza, L. Mundim, H. Nogima, V. Oguri, W.L. Prado Da Silva, A. Santoro, S.M. Silva Do Amaral, A. Sznajder

Instituto de Fisica Teorica, Universidade Estadual Paulista, Sao Paulo, Brazil

C.A. Bernardes², F.A. Dias, T. Dos Anjos Costa², T.R. Fernandez Perez Tomei, E. M. Gregores², C. Lagana, F. Marinho, P.G. Mercadante², S.F. Novaes, Sandra S. Padula

Institute for Nuclear Research and Nuclear Energy, Sofia, Bulgaria

N. Darmenov¹, V. Genchev¹, P. Iaydjiev¹, S. Piperov, M. Rodozov, S. Stoykova, G. Sultanov, V. Tcholakov, R. Trayanov

University of Sofia, Sofia, Bulgaria

A. Dimitrov, R. Hadjiiska, A. Karadzhinova, V. Kozuharov, L. Litov, M. Mateev, B. Pavlov, P. Petkov

Institute of High Energy Physics, Beijing, China

J.G. Bian, G.M. Chen, H.S. Chen, C.H. Jiang, D. Liang, S. Liang, X. Meng, J. Tao, J. Wang, J. Wang, X. Wang, Z. Wang, H. Xiao, M. Xu, J. Zang, Z. Zhang

State Key Lab. of Nucl. Phys. and Tech., Peking University, Beijing, China

Y. Ban, S. Guo, Y. Guo, W. Li, Y. Mao, S.J. Qian, H. Teng, B. Zhu, W. Zou

Universidad de Los Andes, Bogota, Colombia

A. Cabrera, B. Gomez Moreno, A.A. Ocampo Rios, A.F. Osorio Oliveros, J.C. Sanabria

Technical University of Split, Split, Croatia

N. Godinovic, D. Lelas, K. Lelas, R. Plestina³, D. Polic, I. Puljak

University of Split, Split, Croatia

Z. Antunovic, M. Dzelalija

Institute Rudjer Boskovic, Zagreb, Croatia

V. Brigljevic, S. Duric, K. Kadija, S. Morovic

University of Cyprus, Nicosia, Cyprus

A. Attikis, M. Galanti, J. Mousa, C. Nicolaou, F. Ptochos, P.A. Razis

Charles University, Prague, Czech Republic

M. Finger, M. Finger Jr.

Academy of Scientific Research and Technology of the Arab Republic of Egypt, Egyptian Network of High Energy Physics, Cairo, Egypt

Y. Assran⁴, A. Ellithi Kamel, S. Khalil⁵, M.A. Mahmoud⁶

National Institute of Chemical Physics and Biophysics, Tallinn, Estonia

A. Hektor, M. Kadastik, M. Müntel, M. Raidal, L. Rebane, A. Tiko

Department of Physics, University of Helsinki, Helsinki, Finland

V. Azzolini, P. Eerola, G. Fedi

Helsinki Institute of Physics, Helsinki, Finland

S. Czellar, J. Hätkönen, A. Heikkinen, V. Karimäki, R. Kinnunen, M.J. Kortelainen, T. Lampén, K. Lassila-Perini, S. Lehti, T. Lindén, P. Luukka, T. Mäenpää, E. Tuominen, J. Tuominiemi, E. Tuovinen, D. Ungaro, L. Wendland

Lappeenranta University of Technology, Lappeenranta, Finland

K. Banzuzi, A. Karjalainen, A. Korpela, T. Tuuva

Laboratoire d'Annecy-le-Vieux de Physique des Particules, IN2P3-CNRS, Annecy-le-Vieux, France

D. Sillou

DSM/IRFU, CEA/Saclay, Gif-sur-Yvette, France

M. Besancon, S. Choudhury, M. Dejardin, D. Denegri, B. Fabbro, J.L. Faure, F. Ferri, S. Ganjour, F.X. Gentit, A. Givernaud, P. Gras, G. Hamel de Monchenault, P. Jarry, E. Locci, J. Malcles, M. Marionneau, L. Millischer, J. Rander, A. Rosowsky, I. Shreyber, M. Titov, P. Verrecchia

Laboratoire Leprince-Ringuet, Ecole Polytechnique, IN2P3-CNRS, Palaiseau, France

S. Baffioni, F. Beaudette, L. Benhabib, L. Bianchini, M. Bluj⁷, C. Broutin, P. Busson, C. Charlot, T. Dahms, L. Dobrzynski, S. Elgammal, R. Granier de Cassagnac, M. Haguenauer, P. Miné, C. Mironov, C. Ochando, P. Paganini, D. Sabes, R. Salerno, Y. Sirois, C. Thiebaux, B. Wyslouch⁸, A. Zabi

Institut Pluridisciplinaire Hubert Curien, Université de Strasbourg, Université de Haute Alsace Mulhouse, CNRS/IN2P3, Strasbourg, France

J.-L. Agram⁹, J. Andrea, D. Bloch, D. Bodin, J.-M. Brom, M. Cardaci, E.C. Chabert, C. Collard, E. Conte⁹, F. Drouhin⁹, C. Ferro, J.-C. Fontaine⁹, D. Gelé, U. Goerlach, S. Greder, P. Juillot, M. Karim⁹, A.-C. Le Bihan, Y. Mikami, P. Van Hove

Centre de Calcul de l’Institut National de Physique Nucléaire et de Physique des Particules (IN2P3), Villeurbanne, France

F. Fassi, D. Mercier

Université de Lyon, Université Claude Bernard Lyon 1, CNRS-IN2P3, Institut de Physique Nucléaire de Lyon, Villeurbanne, France

C. Baty, S. Beauceron, N. Beaupere, M. Bedjidian, O. Bondu, G. Boudoul, D. Boumediene, H. Brun, J. Chasserat, R. Chierici, D. Contardo, P. Depasse, H. El Mamouni, J. Fay, S. Gascon, B. Ille, T. Kurca, T. Le Grand, M. Lethuillier, L. Mirabito, S. Perries, V. Sordini, S. Tosi, Y. Tschudi, P. Verdier

Institute of High Energy Physics and Informatization, Tbilisi State University, Tbilisi, Georgia

D. Lomidze

RWTH Aachen University, I. Physikalisches Institut, Aachen, Germany

G. Anagnostou, S. Beranek, M. Edelhoff, L. Feld, N. Heracleous, O. Hindrichs, R. Jussen, K. Klein, J. Merz, N. Mohr, A. Ostapchuk, A. Perieanu, F. Raupach, J. Sammet, S. Schael, D. Sprenger, H. Weber, M. Weber, B. Wittmer

RWTH Aachen University, III. Physikalisches Institut A, Aachen, Germany

M. Ata, E. Dietz-Laursonn, M. Erdmann, T. Hebbeker, C. Heidemann, A. Hinzmann, K. Hoepfner, T. Klimkovich, D. Klingebiel, P. Kreuzer, D. Lanske[†], J. Lingemann, C. Magass, M. Merschmeyer, A. Meyer, P. Papacz, H. Pieta, H. Reithler, S.A. Schmitz, L. Sonnenschein, J. Steggemann, D. Teyssier

RWTH Aachen University, III. Physikalisches Institut B, Aachen, Germany

M. Bontenackels, M. Davids, M. Duda, G. Flügge, H. Geenen, M. Giffels, W. Haj Ahmad, D. Heydhausen, F. Hoehle, B. Kargoll, T. Kress, Y. Kuessel, A. Linn, A. Nowack, L. Perchalla, O. Pooth, J. Rennefeld, P. Sauerland, A. Stahl, D. Tornier, M.H. Zoeller

Deutsches Elektronen-Synchrotron, Hamburg, Germany

M. Aldaya Martin, W. Behrenhoff, U. Behrens, M. Bergholz¹⁰, A. Bethani, K. Borras, A. Cakir, A. Campbell, E. Castro, D. Dammann, G. Eckerlin, D. Eckstein, A. Flossdorf, G. Flucke, A. Geiser, J. Hauk, H. Jung¹, M. Kasemann, I. Katkov¹¹, P. Katsas, C. Kleinwort, H. Kluge, A. Knutsson, M. Krämer, D. Krücker, E. Kuznetsova, W. Lange, W. Lohmann¹⁰, R. Mankel, M. Marienfeld, I.-A. Melzer-Pellmann, A.B. Meyer, J. Mnich, A. Mussgiller, J. Olzem, A. Petrukhin, D. Pitzl, A. Raspereza, M. Rosin, R. Schmidt¹⁰, T. Schoerner-Sadenius, N. Sen, A. Spiridonov, M. Stein, J. Tomaszewska, R. Walsh, C. Wissing

University of Hamburg, Hamburg, Germany

C. Autermann, V. Blobel, S. Bobrovskyi, J. Draeger, H. Enderle, U. Gebbert, M. Görner,

T. Hermanns, K. Kaschube, G. Kaussen, H. Kirschenmann, R. Klanner, J. Lange, B. Mura, S. Naumann-Emme, F. Nowak, N. Pietsch, C. Sander, H. Schettler, P. Schleper, E. Schlieckau, M. Schröder, T. Schum, H. Stadie, G. Steinbrück, J. Thomsen

Institut für Experimentelle Kernphysik, Karlsruhe, Germany

C. Barth, J. Bauer, J. Berger, V. Buege, T. Chwalek, W. De Boer, A. Dierlamm, G. Dirkes, M. Feindt, J. Gruschke, C. Hackstein, F. Hartmann, M. Heinrich, H. Held, K.H. Hoffmann, S. Honc, J.R. Komaragiri, T. Kuhr, D. Martschei, S. Mueller, Th. Müller, M. Niegel, O. Oberst, A. Oehler, J. Ott, T. Peiffer, G. Quast, K. Rabbertz, F. Ratnikov, N. Ratnikova, M. Renz, C. Saout, A. Scheurer, P. Schieferdecker, F.-P. Schilling, G. Schott, H.J. Simonis, F.M. Stober, D. Troendle, J. Wagner-Kuhr, T. Weiler, M. Zeise, V. Zhukov¹¹, E.B. Ziebarth

Institute of Nuclear Physics "Demokritos", Aghia Paraskevi, Greece

G. Daskalakis, T. Geralis, S. Kesisoglou, A. Kyriakis, D. Loukas, I. Manolakos, A. Markou, C. Markou, C. Mavrommatis, E. Ntomari, E. Petrakou

University of Athens, Athens, Greece

L. Gouskos, T.J. Mertzimekis, A. Panagiotou, N. Saoulidou, E. Stiliaris

University of Ioánnina, Ioánnina, Greece

I. Evangelou, C. Foudas, P. Kokkas, N. Manthos, I. Papadopoulos, V. Patras, F.A. Triantis

KFKI Research Institute for Particle and Nuclear Physics, Budapest, Hungary

A. Aranyi, G. Bencze, L. Boldizsar, C. Hajdu¹, P. Hidas, D. Horvath¹², A. Kapusi, K. Krajczar¹³, F. Sikler¹, G.I. Veres¹³, G. Vesztregombi¹³

Institute of Nuclear Research ATOMKI, Debrecen, Hungary

N. Beni, J. Molnar, J. Palinkas, Z. Szillasi, V. Veszpremi

University of Debrecen, Debrecen, Hungary

P. Raics, Z.L. Trocsanyi, B. Ujvari

Panjab University, Chandigarh, India

S.B. Beri, V. Bhatnagar, N. Dhingra, R. Gupta, M. Jindal, M. Kaur, J.M. Kohli, M.Z. Mehta, N. Nishu, L.K. Saini, A. Sharma, A.P. Singh, J. Singh, S.P. Singh

University of Delhi, Delhi, India

S. Ahuja, B.C. Choudhary, P. Gupta, S. Jain, A. Kumar, A. Kumar, M. Naimuddin, K. Ranjan, R.K. Shivpuri

Saha Institute of Nuclear Physics, Kolkata, India

S. Banerjee, S. Bhattacharya, S. Dutta, B. Gomber, S. Jain, R. Khurana, S. Sarkar

Bhabha Atomic Research Centre, Mumbai, India

R.K. Choudhury, D. Dutta, S. Kailas, V. Kumar, P. Mehta, A.K. Mohanty¹, L.M. Pant, P. Shukla

Tata Institute of Fundamental Research - EHEP, Mumbai, India

T. Aziz, M. Guchait¹⁴, A. Gurtu, M. Maity¹⁵, D. Majumder, G. Majumder, K. Mazumdar, G.B. Mohanty, A. Saha, K. Sudhakar, N. Wickramage

Tata Institute of Fundamental Research - HEGR, Mumbai, India

S. Banerjee, S. Dugad, N.K. Mondal

Institute for Research and Fundamental Sciences (IPM), Tehran, Iran

H. Arfaei, H. Bakhshiansohi¹⁶, S.M. Etesami, A. Fahim¹⁶, M. Hashemi, H. Hesari, A. Jafari¹⁶,

M. Khakzad, A. Mohammadi¹⁷, M. Mohammadi Najafabadi, S. Paktinat Mehdiabadi, B. Safarzadeh, M. Zeinali¹⁸

INFN Sezione di Bari ^a, Università di Bari ^b, Politecnico di Bari ^c, Bari, Italy

M. Abbrescia^{a,b}, L. Barbone^{a,b}, C. Calabria^{a,b}, A. Colaleo^a, D. Creanza^{a,c}, N. De Filippis^{a,c,1}, M. De Palma^{a,b}, L. Fiore^a, G. Iaselli^{a,c}, L. Lusito^{a,b}, G. Maggi^{a,c}, M. Maggi^a, N. Manna^{a,b}, B. Marangelli^{a,b}, S. My^{a,c}, S. Nuzzo^{a,b}, N. Pacifico^{a,b}, G.A. Pierro^a, A. Pompili^{a,b}, G. Pugliese^{a,c}, F. Romano^{a,c}, G. Roselli^{a,b}, G. Selvaggi^{a,b}, L. Silvestris^a, R. Trentadue^a, S. Tupputi^{a,b}, G. Zito^a

INFN Sezione di Bologna ^a, Università di Bologna ^b, Bologna, Italy

G. Abbiendi^a, A.C. Benvenuti^a, D. Bonacorsi^a, S. Braibant-Giacomelli^{a,b}, L. Brigliadori^a, P. Capiluppi^{a,b}, A. Castro^{a,b}, F.R. Cavallo^a, M. Cuffiani^{a,b}, G.M. Dallavalle^a, F. Fabbri^a, A. Fanfani^{a,b}, D. Fasanella^a, P. Giacomelli^a, M. Giunta^a, C. Grandi^a, S. Marcellini^a, G. Masetti^b, M. Meneghelli^{a,b}, A. Montanari^a, F.L. Navarria^{a,b}, F. Odorici^a, A. Perrotta^a, F. Primavera^a, A.M. Rossi^{a,b}, T. Rovelli^{a,b}, G. Siroli^{a,b}, R. Travaglini^{a,b}

INFN Sezione di Catania ^a, Università di Catania ^b, Catania, Italy

S. Albergo^{a,b}, G. Cappello^{a,b}, M. Chiorboli^{a,b,1}, S. Costa^{a,b}, R. Potenza^{a,b}, A. Tricomi^{a,b}, C. Tuve^{a,b}

INFN Sezione di Firenze ^a, Università di Firenze ^b, Firenze, Italy

G. Barbagli^a, V. Ciulli^{a,b}, C. Civinini^a, R. D'Alessandro^{a,b}, E. Focardi^{a,b}, S. Frosali^{a,b}, E. Gallo^a, S. Gonzi^{a,b}, P. Lenzi^{a,b}, M. Meschini^a, S. Paoletti^a, G. Sguazzoni^a, A. Tropiano^{a,1}

INFN Laboratori Nazionali di Frascati, Frascati, Italy

L. Benussi, S. Bianco, S. Colafranceschi¹⁹, F. Fabbri, D. Piccolo

INFN Sezione di Genova, Genova, Italy

P. Fabbricatore, R. Musenich

INFN Sezione di Milano-Bicocca ^a, Università di Milano-Bicocca ^b, Milano, Italy

A. Benaglia^{a,b}, F. De Guio^{a,b,1}, L. Di Matteo^{a,b}, S. Gennai¹, A. Ghezzi^{a,b}, S. Malvezzi^a, A. Martelli^{a,b}, A. Massironi^{a,b}, D. Menasce^a, L. Moroni^a, M. Paganoni^{a,b}, D. Pedrini^a, S. Ragazzi^{a,b}, N. Redaelli^a, S. Sala^a, T. Tabarelli de Fatis^{a,b}

INFN Sezione di Napoli ^a, Università di Napoli "Federico II" ^b, Napoli, Italy

S. Buontempo^a, C.A. Carrillo Montoya^{a,1}, N. Cavallo^{a,20}, A. De Cosa^{a,b}, F. Fabozzi^{a,20}, A.O.M. Iorio^{a,1}, L. Lista^a, M. Merola^{a,b}, P. Paolucci^a

INFN Sezione di Padova ^a, Università di Padova ^b, Università di Trento (Trento) ^c, Padova, Italy

P. Azzi^a, N. Bacchetta^a, P. Bellan^{a,b}, D. Bisello^{a,b}, A. Branca^a, R. Carlin^{a,b}, P. Checchia^a, T. Dorigo^a, U. Dosselli^a, F. Fanzago^a, F. Gasparini^{a,b}, U. Gasparini^{a,b}, A. Gozzelino, S. Lacaprara^{a,21}, I. Lazzizzeri^{a,c}, M. Margoni^{a,b}, M. Mazzucato^a, A.T. Meneguzzo^{a,b}, M. Nespolo^{a,1}, L. Perrozzi^{a,1}, N. Pozzobon^{a,b}, P. Ronchese^{a,b}, F. Simonetto^{a,b}, E. Torassa^a, M. Tosi^{a,b}, S. Vanini^{a,b}, P. Zotto^{a,b}, G. Zumerle^{a,b}

INFN Sezione di Pavia ^a, Università di Pavia ^b, Pavia, Italy

P. Baesso^{a,b}, U. Berzano^a, S.P. Ratti^{a,b}, C. Riccardi^{a,b}, P. Torre^{a,b}, P. Vitulo^{a,b}, C. Viviani^{a,b}

INFN Sezione di Perugia ^a, Università di Perugia ^b, Perugia, Italy

M. Biasini^{a,b}, G.M. Bilei^a, B. Caponeri^{a,b}, L. Fanò^{a,b}, P. Lariccia^{a,b}, A. Lucaroni^{a,b,1}, G. Mantovani^{a,b}, M. Menichelli^a, A. Nappi^{a,b}, F. Romeo^{a,b}, A. Santocchia^{a,b}, S. Taroni^{a,b,1}, M. Valdata^{a,b}

INFN Sezione di Pisa ^a, Università di Pisa ^b, Scuola Normale Superiore di Pisa ^c, Pisa, Italy
 P. Azzurri^{a,c}, G. Bagliesi^a, J. Bernardini^{a,b}, T. Boccali^{a,1}, G. Broccolo^{a,c}, R. Castaldi^a,
 R.T. D'Agnolo^{a,c}, R. Dell'Orso^a, F. Fiori^{a,b}, L. Foà^{a,c}, A. Giassi^a, A. Kraan^a, F. Ligabue^{a,c},
 T. Lomtadze^a, L. Martini^{a,22}, A. Messineo^{a,b}, F. Palla^a, F. Palmonari, G. Segneri^a, A.T. Serban^a,
 P. Spagnolo^a, R. Tenchini^a, G. Tonelli^{a,b,1}, A. Venturi^{a,1}, P.G. Verdini^a

INFN Sezione di Roma ^a, Università di Roma "La Sapienza" ^b, Roma, Italy

L. Barone^{a,b}, F. Cavallari^a, D. Del Re^{a,b}, E. Di Marco^{a,b}, M. Diemoz^a, D. Franci^{a,b}, M. Grassi^{a,1},
 E. Longo^{a,b}, P. Meridiani, S. Nourbakhsh^a, G. Organtini^{a,b}, F. Pandolfi^{a,b,1}, R. Paramatti^a,
 S. Rahatlou^{a,b}, C. Rovelli¹

INFN Sezione di Torino ^a, Università di Torino ^b, Università del Piemonte Orientale (Novara) ^c, Torino, Italy

N. Amapane^{a,b}, R. Arcidiacono^{a,c}, S. Argiro^{a,b}, M. Arneodo^{a,c}, C. Biino^a, C. Botta^{a,b,1},
 N. Cartiglia^a, R. Castello^{a,b}, M. Costa^{a,b}, N. Demaria^a, A. Graziano^{a,b,1}, C. Mariotti^a,
 M. Marone^{a,b}, S. Maselli^a, E. Migliore^{a,b}, G. Mila^{a,b}, V. Monaco^{a,b}, M. Musich^a,
 M.M. Obertino^{a,c}, N. Pastrone^a, M. Pelliccioni^{a,b}, A. Potenza^{a,b}, A. Romero^{a,b}, M. Ruspa^{a,c},
 R. Sacchi^{a,b}, V. Sola^{a,b}, A. Solano^{a,b}, A. Staiano^a, A. Vilela Pereira^a

INFN Sezione di Trieste ^a, Università di Trieste ^b, Trieste, Italy

S. Belforte^a, F. Cossutti^a, G. Della Ricca^{a,b}, B. Gobbo^a, D. Montanino^{a,b}, A. Penzo^a

Kangwon National University, Chunchon, Korea

S.G. Heo, S.K. Nam

Kyungpook National University, Daegu, Korea

S. Chang, J. Chung, D.H. Kim, G.N. Kim, J.E. Kim, D.J. Kong, H. Park, S.R. Ro, D.C. Son, T. Son

Chonnam National University, Institute for Universe and Elementary Particles, Kwangju, Korea

Zero Kim, J.Y. Kim, S. Song

Korea University, Seoul, Korea

S. Choi, B. Hong, M. Jo, H. Kim, J.H. Kim, T.J. Kim, K.S. Lee, D.H. Moon, S.K. Park, K.S. Sim

University of Seoul, Seoul, Korea

M. Choi, S. Kang, H. Kim, C. Park, I.C. Park, S. Park, G. Ryu

Sungkyunkwan University, Suwon, Korea

Y. Choi, Y.K. Choi, J. Goh, M.S. Kim, B. Lee, J. Lee, S. Lee, H. Seo, I. Yu

Vilnius University, Vilnius, Lithuania

M.J. Bilinskas, I. Grigelionis, M. Janulis, D. Martisiute, P. Petrov, M. Polujanskas, T. Sabonis

Centro de Investigacion y de Estudios Avanzados del IPN, Mexico City, Mexico

H. Castilla-Valdez, E. De La Cruz-Burelo, I. Heredia-de La Cruz, R. Lopez-Fernandez,
 R. Magaña Villalba, A. Sánchez-Hernández, L.M. Villasenor-Cendejas

Universidad Iberoamericana, Mexico City, Mexico

S. Carrillo Moreno, F. Vazquez Valencia

Benemerita Universidad Autonoma de Puebla, Puebla, Mexico

H.A. Salazar Ibarguen

Universidad Autónoma de San Luis Potosí, San Luis Potosí, Mexico

E. Casimiro Linares, A. Morelos Pineda, M.A. Reyes-Santos

University of Auckland, Auckland, New Zealand
D. Kofcheck, J. Tam

University of Canterbury, Christchurch, New Zealand
P.H. Butler, R. Doesburg, H. Silverwood

National Centre for Physics, Quaid-I-Azam University, Islamabad, Pakistan
M. Ahmad, I. Ahmed, M.I. Asghar, H.R. Hoorani, S. Khalid, W.A. Khan, T. Khurshid, S. Qazi, M.A. Shah

Institute of Experimental Physics, Faculty of Physics, University of Warsaw, Warsaw, Poland
G. Brona, M. Cwiok, W. Dominik, K. Doroba, A. Kalinowski, M. Konecki, J. Krolikowski

Soltan Institute for Nuclear Studies, Warsaw, Poland
T. Frueboes, R. Gokieli, M. Górska, M. Kazana, K. Nawrocki, K. Romanowska-Rybinska, M. Szleper, G. Wrochna, P. Zalewski

Laboratório de Instrumentação e Física Experimental de Partículas, Lisboa, Portugal
N. Almeida, P. Bargassa, A. David, P. Faccioli, P.G. Ferreira Parracho, M. Gallinaro¹, P. Musella, A. Nayak, J. Pela¹, P.Q. Ribeiro, J. Seixas, J. Varela

Joint Institute for Nuclear Research, Dubna, Russia
S. Afanasiev, I. Belotelov, P. Bunin, I. Golutvin, V. Karjavin, G. Kozlov, A. Lanev, P. Moisenz, V. Palichik, V. Perelygin, M. Savina, S. Shmatov, V. Smirnov, A. Volodko, A. Zarubin

Petersburg Nuclear Physics Institute, Gatchina (St Petersburg), Russia
V. Golovtsov, Y. Ivanov, V. Kim, P. Levchenko, V. Murzin, V. Oreshkin, I. Smirnov, V. Sulimov, L. Uvarov, S. Vavilov, A. Vorobyev, An. Vorobyev

Institute for Nuclear Research, Moscow, Russia
Yu. Andreev, A. Dermenev, S. Glinenko, N. Golubev, M. Kirsanov, N. Krasnikov, V. Matveev, A. Pashenkov, A. Toropin, S. Troitsky

Institute for Theoretical and Experimental Physics, Moscow, Russia
V. Epshteyn, V. Gavrilov, V. Kaftanov[†], M. Kossov¹, A. Krokhotin, N. Lychkovskaya, V. Popov, G. Safronov, S. Semenov, V. Stolin, E. Vlasov, A. Zhokin

Moscow State University, Moscow, Russia
A. Belyaev, E. Boos, M. Dubinin²³, L. Dudko, A. Ershov, A. Gribushin, O. Kodolova, I. Loktin, A. Markina, S. Obraztsov, M. Perfilov, S. Petrushanko, L. Sarycheva, V. Savrin, A. Snigirev

P.N. Lebedev Physical Institute, Moscow, Russia
V. Andreev, M. Azarkin, I. Dremin, M. Kirakosyan, A. Leonidov, S.V. Rusakov, A. Vinogradov

State Research Center of Russian Federation, Institute for High Energy Physics, Protvino, Russia

I. Azhgirey, I. Bayshev, S. Bitioukov, V. Grishin¹, V. Kachanov, D. Konstantinov, A. Korablev, V. Krychkine, V. Petrov, R. Ryutin, A. Sobol, L. Tourtchanovitch, S. Troshin, N. Tyurin, A. Uzunian, A. Volkov

University of Belgrade, Faculty of Physics and Vinca Institute of Nuclear Sciences, Belgrade, Serbia

P. Adzic²⁴, M. Djordjevic, D. Krpic²⁴, J. Milosevic

Centro de Investigaciones Energéticas Medioambientales y Tecnológicas (CIEMAT), Madrid, Spain

M. Aguilar-Benitez, J. Alcaraz Maestre, P. Arce, C. Battilana, E. Calvo, M. Cepeda, M. Cerrada, M. Chamizo Llatas, N. Colino, B. De La Cruz, A. Delgado Peris, C. Diez Pardos, D. Domínguez Vázquez, C. Fernandez Bedoya, J.P. Fernández Ramos, A. Ferrando, J. Flix, M.C. Fouz, P. Garcia-Abia, O. Gonzalez Lopez, S. Goy Lopez, J.M. Hernandez, M.I. Josa, G. Merino, J. Puerta Pelayo, I. Redondo, L. Romero, J. Santaolalla, M.S. Soares, C. Willmott

Universidad Autónoma de Madrid, Madrid, Spain

C. Albajar, G. Codispoti, J.F. de Trocóniz

Universidad de Oviedo, Oviedo, Spain

J. Cuevas, J. Fernandez Menendez, S. Folgueras, I. Gonzalez Caballero, L. Lloret Iglesias, J.M. Vizan Garcia

Instituto de Física de Cantabria (IFCA), CSIC-Universidad de Cantabria, Santander, Spain

J.A. Brochero Cifuentes, I.J. Cabrillo, A. Calderon, S.H. Chuang, J. Duarte Campderros, M. Felcini²⁵, M. Fernandez, G. Gomez, J. Gonzalez Sanchez, C. Jorda, P. Lobelle Pardo, A. Lopez Virto, J. Marco, R. Marco, C. Martinez Rivero, F. Matorras, F.J. Munoz Sanchez, J. Piedra Gomez²⁶, T. Rodrigo, A.Y. Rodríguez-Marrero, A. Ruiz-Jimeno, L. Scodellaro, M. Sobron Sanudo, I. Vila, R. Vilar Cortabitarte

CERN, European Organization for Nuclear Research, Geneva, Switzerland

D. Abbaneo, E. Auffray, G. Auzinger, P. Baillon, A.H. Ball, D. Barney, A.J. Bell²⁷, D. Benedetti, C. Bernet³, W. Bialas, P. Bloch, A. Bocci, S. Bolognesi, M. Bona, H. Breuker, K. Bunkowski, T. Camporesi, G. Cerminara, T. Christiansen, J.A. Coarasa Perez, B. Curé, D. D'Enterria, A. De Roeck, S. Di Guida, N. Dupont-Sagorin, A. Elliott-Peisert, B. Frisch, W. Funk, A. Gaddi, G. Georgiou, H. Gerwig, D. Gigi, K. Gill, D. Giordano, F. Glege, R. Gomez-Reino Garrido, M. Gouzevitch, P. Govoni, S. Gowdy, L. Guiducci, M. Hansen, C. Hartl, J. Harvey, J. Hegeman, B. Hegner, H.F. Hoffmann, A. Honma, V. Innocente, P. Janot, K. Kaadze, E. Karavakis, P. Lecoq, C. Lourenço, T. Mäki, M. Malberti, L. Malgeri, M. Mannelli, L. Masetti, A. Maurisset, F. Meijers, S. Mersi, E. Meschi, R. Moser, M.U. Mozer, M. Mulders, E. Nesvold¹, M. Nguyen, T. Orimoto, L. Orsini, E. Palencia Cortezon, E. Perez, A. Petrilli, A. Pfeiffer, M. Pierini, M. Pimiä, D. Piparo, G. Polese, A. Racz, W. Reece, J. Rodrigues Antunes, G. Rolandi²⁸, T. Rommerskirchen, M. Rovere, H. Sakulin, C. Schäfer, C. Schwick, I. Segoni, A. Sharma, P. Siegrist, P. Silva, M. Simon, P. Sphicas²⁹, M. Spiropulu²³, M. Stoye, P. Tropea, A. Tsirou, P. Vichoudis, M. Voutilainen, W.D. Zeuner

Paul Scherrer Institut, Villigen, Switzerland

W. Bertl, K. Deiters, W. Erdmann, K. Gabathuler, R. Horisberger, Q. Ingram, H.C. Kaestli, S. König, D. Kotlinski, U. Langenegger, F. Meier, D. Renker, T. Rohe, J. Sibille³⁰, A. Starodumov³¹

Institute for Particle Physics, ETH Zurich, Zurich, Switzerland

L. Bäni, P. Bortignon, L. Caminada³², B. Casal, N. Chanon, Z. Chen, S. Cittolin, G. Dissertori, M. Dittmar, J. Eugster, K. Freudeneich, C. Grab, W. Hintz, P. Lecomte, W. Lustermann, C. Marchica³², P. Martinez Ruiz del Arbol, P. Milenovic³³, F. Moortgat, C. Nägeli³², P. Nef, F. Nessi-Tedaldi, L. Pape, F. Pauss, T. Punz, A. Rizzi, F.J. Ronga, M. Rossini, L. Sala, A.K. Sanchez, M.-C. Sawley, B. Stieger, L. Tauscher[†], A. Thea, K. Theofilatos, D. Treille, C. Urscheler, R. Wallny, M. Weber, L. Wehrli, J. Weng

Universität Zürich, Zurich, Switzerland

E. Aguiló, C. Amsler, V. Chiochia, S. De Visscher, C. Favaro, M. Ivova Rikova, B. Millan Mejias, P. Otiougova, P. Robmann, A. Schmidt, H. Snoek

National Central University, Chung-Li, Taiwan

Y.H. Chang, K.H. Chen, C.M. Kuo, S.W. Li, W. Lin, Z.K. Liu, Y.J. Lu, D. Mekterovic, R. Volpe, J.H. Wu, S.S. Yu

National Taiwan University (NTU), Taipei, Taiwan

P. Bartalini, P. Chang, Y.H. Chang, Y.W. Chang, Y. Chao, K.F. Chen, W.-S. Hou, Y. Hsiung, K.Y. Kao, Y.J. Lei, R.-S. Lu, J.G. Shiu, Y.M. Tzeng, X. Wan, M. Wang

Cukurova University, Adana, Turkey

A. Adiguzel, M.N. Bakirci³⁴, S. Cerci³⁵, C. Dozen, I. Dumanoglu, E. Eskut, S. Girgis, G. Gokbulut, I. Hos, E.E. Kangal, A. Kayis Topaksu, G. Onengut, K. Ozdemir, S. Ozturk³⁶, A. Polatoz, K. Sogut³⁷, D. Sunar Cerci³⁵, B. Tali³⁵, H. Topakli³⁴, D. Uzun, L.N. Vergili, M. Vergili

Middle East Technical University, Physics Department, Ankara, Turkey

I.V. Akin, T. Aliev, B. Bilin, S. Bilmis, M. Deniz, H. Gamsizkan, A.M. Guler, K. Ocalan, A. Ozpineci, M. Serin, R. Sever, U.E. Surat, M. Yalvac, E. Yildirim, M. Zeyrek

Bogazici University, Istanbul, Turkey

M. Deliomeroglu, D. Demir³⁸, E. Gülmез, B. Isildak, M. Kaya³⁹, O. Kaya³⁹, M. Özbek, S. Ozkorucuklu⁴⁰, N. Sonmez⁴¹

National Scientific Center, Kharkov Institute of Physics and Technology, Kharkov, Ukraine

L. Levchuk

University of Bristol, Bristol, United Kingdom

F. Bostock, J.J. Brooke, T.L. Cheng, E. Clement, D. Cussans, R. Frazier, J. Goldstein, M. Grimes, D. Hartley, G.P. Heath, H.F. Heath, L. Kreczko, S. Metson, D.M. Newbold⁴², K. Nirunpong, A. Poll, S. Senkin, V.J. Smith

Rutherford Appleton Laboratory, Didcot, United Kingdom

L. Basso⁴³, K.W. Bell, A. Belyaev⁴³, C. Brew, R.M. Brown, B. Camanzi, D.J.A. Cockerill, J.A. Coughlan, K. Harder, S. Harper, J. Jackson, B.W. Kennedy, E. Olaiya, D. Petyt, B.C. Radburn-Smith, C.H. Shepherd-Themistocleous, I.R. Tomalin, W.J. Womersley, S.D. Worm

Imperial College, London, United Kingdom

R. Bainbridge, G. Ball, J. Ballin, R. Beuselinck, O. Buchmuller, D. Colling, N. Cripps, M. Cutajar, G. Davies, M. Della Negra, W. Ferguson, J. Fulcher, D. Futyan, A. Gilbert, A. Guneratne Bryer, G. Hall, Z. Hatherell, J. Hays, G. Iles, M. Jarvis, G. Karapostoli, L. Lyons, B.C. MacEvoy, A.-M. Magnan, J. Marrouche, B. Mathias, R. Nandi, J. Nash, A. Nikitenko³¹, A. Papageorgiou, M. Pesaresi, K. Petridis, M. Pioppi⁴⁴, D.M. Raymond, S. Rogerson, N. Rompotis, A. Rose, M.J. Ryan, C. Seez, P. Sharp, A. Sparrow, A. Tapper, S. Tourneur, M. Vazquez Acosta, T. Virdee, S. Wakefield, N. Wardle, D. Wardrope, T. Whyntie

Brunel University, Uxbridge, United Kingdom

M. Barrett, M. Chadwick, J.E. Cole, P.R. Hobson, A. Khan, P. Kyberd, D. Leslie, W. Martin, I.D. Reid, L. Teodorescu

Baylor University, Waco, USA

K. Hatakeyama, H. Liu

The University of Alabama, Tuscaloosa, USA

C. Henderson

Boston University, Boston, USA

T. Bose, E. Carrera Jarrin, C. Fantasia, A. Heister, J. St. John, P. Lawson, D. Lazic, J. Rohlf, D. Sperka, L. Sulak

Brown University, Providence, USA

A. Avetisyan, S. Bhattacharya, J.P. Chou, D. Cutts, A. Ferapontov, U. Heintz, S. Jabeen, G. Kukartsev, G. Landsberg, M. Luk, M. Narain, D. Nguyen, M. Segala, T. Sinthuprasith, T. Speer, K.V. Tsang

University of California, Davis, Davis, USA

R. Breedon, G. Breto, M. Calderon De La Barca Sanchez, S. Chauhan, M. Chertok, J. Conway, P.T. Cox, J. Dolen, R. Erbacher, E. Friis, W. Ko, A. Kopecky, R. Lander, H. Liu, S. Maruyama, T. Miceli, M. Nikolic, D. Pellett, J. Robles, B. Rutherford, S. Salur, T. Schwarz, M. Searle, J. Smith, M. Squires, M. Tripathi, R. Vasquez Sierra, C. Veelken

University of California, Los Angeles, Los Angeles, USA

V. Andreev, K. Arisaka, D. Cline, R. Cousins, A. Deisher, J. Duris, S. Erhan, C. Farrell, J. Hauser, M. Ignatenko, C. Jarvis, C. Plager, G. Rakness, P. Schlein[†], J. Tucker, V. Valuev

University of California, Riverside, Riverside, USA

J. Babb, A. Chandra, R. Clare, J. Ellison, J.W. Gary, F. Giordano, G. Hanson, G.Y. Jeng, S.C. Kao, F. Liu, H. Liu, O.R. Long, A. Luthra, H. Nguyen, S. Paramesvaran, B.C. Shen[†], R. Stringer, J. Sturdy, S. Sumowidagdo, R. Wilken, S. Wimpenny

University of California, San Diego, La Jolla, USA

W. Andrews, J.G. Branson, G.B. Cerati, D. Evans, F. Golf, A. Holzner, R. Kelley, M. Lebourgeois, J. Letts, B. Mangano, S. Padhi, C. Palmer, G. Petrucciani, H. Pi, M. Pieri, R. Ranieri, M. Sani, V. Sharma, S. Simon, E. Sudano, M. Tadel, Y. Tu, A. Vartak, S. Wasserbaech⁴⁵, F. Würthwein, A. Yagil, J. Yoo

University of California, Santa Barbara, Santa Barbara, USA

D. Barge, R. Bellan, C. Campagnari, M. D'Alfonso, T. Danielson, K. Flowers, P. Geffert, J. Incandela, C. Justus, P. Kalavase, S.A. Koay, D. Kovalskyi, V. Krutelyov, S. Lowette, N. Mccoll, V. Pavlunin, F. Rebassoo, J. Ribnik, J. Richman, R. Rossin, D. Stuart, W. To, J.R. Vlimant

California Institute of Technology, Pasadena, USA

A. Apresyan, A. Bornheim, J. Bunn, Y. Chen, M. Gataullin, Y. Ma, A. Mott, H.B. Newman, C. Rogan, K. Shin, V. Timciuc, P. Traczyk, J. Veverka, R. Wilkinson, Y. Yang, R.Y. Zhu

Carnegie Mellon University, Pittsburgh, USA

B. Akgun, R. Carroll, T. Ferguson, Y. Iiyama, D.W. Jang, S.Y. Jun, Y.F. Liu, M. Paulini, J. Russ, H. Vogel, I. Vorobiev

University of Colorado at Boulder, Boulder, USA

J.P. Cumalat, M.E. Dinardo, B.R. Drell, C.J. Edelmaier, W.T. Ford, A. Gaz, B. Heyburn, E. Luiggi Lopez, U. Nauenberg, J.G. Smith, K. Stenson, K.A. Ulmer, S.R. Wagner, S.L. Zang

Cornell University, Ithaca, USA

L. Agostino, J. Alexander, A. Chatterjee, N. Eggert, L.K. Gibbons, B. Heltsley, K. Henriksson, W. Hopkins, A. Khukhunaishvili, B. Kreis, Y. Liu, G. Nicolas Kaufman, J.R. Patterson, D. Puigh, A. Ryd, M. Saelim, E. Salvati, X. Shi, W. Sun, W.D. Teo, J. Thom, J. Thompson, J. Vaughan, Y. Weng, L. Winstrom, P. Wittich

Fairfield University, Fairfield, USA

A. Biselli, G. Cirino, D. Winn

Fermi National Accelerator Laboratory, Batavia, USA

S. Abdullin, M. Albrow, J. Anderson, G. Apollinari, M. Atac, J.A. Bakken, L.A.T. Bauerick, A. Beretvas, J. Berryhill, P.C. Bhat, I. Bloch, F. Borcherding, K. Burkett, J.N. Butler, V. Chetluru, H.W.K. Cheung, F. Chlebana, S. Cihangir, W. Cooper, D.P. Eartly, V.D. Elvira, S. Esen, I. Fisk, J. Freeman, Y. Gao, E. Gottschalk, D. Green, K. Gunthoti, O. Gutsche, J. Hanlon, R.M. Harris, J. Hirschauer, B. Hooberman, H. Jensen, M. Johnson, U. Joshi, R. Khatiwada, B. Klima, K. Kousouris, S. Kunori, S. Kwan, C. Leonidopoulos, P. Limon, D. Lincoln, R. Lipton, J. Lykken, K. Maeshima, J.M. Marraffino, D. Mason, P. McBride, T. Miao, K. Mishra, S. Mrenna, Y. Musienko⁴⁶, C. Newman-Holmes, V. O'Dell, J. Pivarski, R. Pordes, O. Prokofyev, E. Sexton-Kennedy, S. Sharma, W.J. Spalding, L. Spiegel, P. Tan, L. Taylor, S. Tkaczyk, L. Uplegger, E.W. Vaandering, R. Vidal, J. Whitmore, W. Wu, F. Yumiceva, J.C. Yun

University of Florida, Gainesville, USA

D. Acosta, P. Avery, D. Bourilkov, M. Chen, S. Das, M. De Gruttola, G.P. Di Giovanni, D. Dobur, A. Drozdetskiy, R.D. Field, M. Fisher, Y. Fu, I.K. Furic, J. Gartner, J. Hugon, B. Kim, J. Konigsberg, A. Korytov, A. Kropivnitskaya, T. Kypreos, J.F. Low, K. Matchev, G. Mitselmakher, L. Muniz, C. Prescott, R. Remington, A. Rinkevicius, M. Schmitt, B. Scurlock, P. Sellers, N. Skhirtladze, M. Snowball, D. Wang, J. Yelton, M. Zakaria

Florida International University, Miami, USA

V. Gaultney, L.M. Lebolo, S. Linn, P. Markowitz, G. Martinez, J.L. Rodriguez

Florida State University, Tallahassee, USA

T. Adams, A. Askew, J. Bochenek, J. Chen, B. Diamond, S.V. Gleyzer, J. Haas, S. Hagopian, V. Hagopian, M. Jenkins, K.F. Johnson, H. Prosper, L. Quertenmont, S. Sekmen, V. Veeraraghavan

Florida Institute of Technology, Melbourne, USA

M.M. Baarmann, B. Dorney, S. Guragain, M. Hohlmann, H. Kalakhety, I. Vodopiyanov

University of Illinois at Chicago (UIC), Chicago, USA

M.R. Adams, I.M. Anghel, L. Apanasevich, Y. Bai, V.E. Bazterra, R.R. Betts, J. Callner, R. Cavanaugh, C. Dragoiu, L. Gauthier, C.E. Gerber, D.J. Hofman, S. Khalatyan, G.J. Kunde⁴⁷, F. Lacroix, M. Malek, C. O'Brien, C. Silkworth, C. Silvestre, A. Smoron, D. Strom, N. Varelas

The University of Iowa, Iowa City, USA

U. Akgun, E.A. Albayrak, B. Bilki, W. Clarida, F. Duru, C.K. Lae, E. McCliment, J.-P. Merlo, H. Mermerkaya⁴⁸, A. Mestvirishvili, A. Moeller, J. Nachtman, C.R. Newsom, E. Norbeck, J. Olson, Y. Onel, F. Ozok, S. Sen, J. Wetzel, T. Yetkin, K. Yi

Johns Hopkins University, Baltimore, USA

B.A. Barnett, B. Blumenfeld, A. Bonato, C. Eskew, D. Fehling, G. Giurgiu, A.V. Gritsan, Z.J. Guo, G. Hu, P. Maksimovic, S. Rappoccio, M. Swartz, N.V. Tran, A. Whitbeck

The University of Kansas, Lawrence, USA

P. Baringer, A. Bean, G. Benelli, O. Grachov, R.P. Kenny Iii, M. Murray, D. Noonan, S. Sanders, J.S. Wood, V. Zhukova

Kansas State University, Manhattan, USA

A.f. Barfuss, T. Bolton, I. Chakaberia, A. Ivanov, S. Khalil, M. Makouski, Y. Maravin, S. Shrestha, I. Svintradze, Z. Wan

Lawrence Livermore National Laboratory, Livermore, USA

J. Gronberg, D. Lange, D. Wright

University of Maryland, College Park, USA

A. Baden, M. Boutemeur, S.C. Eno, D. Ferencek, J.A. Gomez, N.J. Hadley, R.G. Kellogg, M. Kirn, Y. Lu, A.C. Mignerey, K. Rossato, P. Rumerio, F. Santanastasio, A. Skuja, J. Temple, M.B. Tonjes, S.C. Tonwar, E. Twedt

Massachusetts Institute of Technology, Cambridge, USA

B. Alver, G. Bauer, J. Bendavid, W. Busza, E. Butz, I.A. Cali, M. Chan, V. Dutta, P. Everaerts, G. Gomez Ceballos, M. Goncharov, K.A. Hahn, P. Harris, Y. Kim, M. Klute, Y.-J. Lee, W. Li, C. Loizides, P.D. Luckey, T. Ma, S. Nahm, C. Paus, D. Ralph, C. Roland, G. Roland, M. Rudolph, G.S.F. Stephans, F. Stöckli, K. Sumorok, K. Sung, D. Velicanu, E.A. Wenger, R. Wolf, S. Xie, M. Yang, Y. Yilmaz, A.S. Yoon, M. Zanetti

University of Minnesota, Minneapolis, USA

S.I. Cooper, P. Cushman, B. Dahmes, A. De Benedetti, P.R. Dudero, G. Franzoni, A. Gude, J. Haupt, K. Klaoetke, Y. Kubota, J. Mans, N. Pastika, V. Rekovic, R. Rusack, M. Sashevile, A. Singovsky, N. Tambe

University of Mississippi, University, USA

L.M. Cremaldi, R. Godang, R. Kroeger, L. Perera, R. Rahmat, D.A. Sanders, D. Summers

University of Nebraska-Lincoln, Lincoln, USA

K. Bloom, S. Bose, J. Butt, D.R. Claes, A. Dominguez, M. Eads, P. Jindal, J. Keller, T. Kelly, I. Kravchenko, J. Lazo-Flores, H. Malbouisson, S. Malik, G.R. Snow

State University of New York at Buffalo, Buffalo, USA

U. Baur, A. Godshalk, I. Iashvili, S. Jain, A. Kharchilava, A. Kumar, S.P. Shipkowski, K. Smith

Northeastern University, Boston, USA

G. Alverson, E. Barberis, D. Baumgartel, O. Boeriu, M. Chasco, S. Reucroft, J. Swain, D. Trocino, D. Wood, J. Zhang

Northwestern University, Evanston, USA

A. Anastassov, A. Kubik, N. Odell, R.A. Ofierzynski, B. Pollack, A. Pozdnyakov, M. Schmitt, S. Stoynev, M. Velasco, S. Won

University of Notre Dame, Notre Dame, USA

L. Antonelli, D. Berry, A. Brinkerhoff, M. Hildreth, C. Jessop, D.J. Karmgard, J. Kolb, T. Kolberg, K. Lannon, W. Luo, S. Lynch, N. Marinelli, D.M. Morse, T. Pearson, R. Ruchti, J. Slaunwhite, N. Valls, M. Wayne, J. Ziegler

The Ohio State University, Columbus, USA

B. Bylsma, L.S. Durkin, J. Gu, C. Hill, P. Killewald, K. Kotov, T.Y. Ling, M. Rodenburg, C. Vuosalo, G. Williams

Princeton University, Princeton, USA

N. Adam, E. Berry, P. Elmer, D. Gerbaudo, V. Halyo, P. Hebda, A. Hunt, E. Laird, D. Lopes Pegna, D. Marlow, T. Medvedeva, M. Mooney, J. Olsen, P. Piroué, X. Quan, B. Safdi, H. Saka, D. Stickland, C. Tully, J.S. Werner, A. Zuranski

University of Puerto Rico, Mayaguez, USA

J.G. Acosta, X.T. Huang, A. Lopez, H. Mendez, S. Oliveros, J.E. Ramirez Vargas, A. Zatserklyaniy

Purdue University, West Lafayette, USA

E. Alagoz, V.E. Barnes, G. Bolla, L. Borrello, D. Bortoletto, M. De Mattia, A. Everett,

A.F. Garfinkel, L. Gutay, Z. Hu, M. Jones, O. Koybasi, M. Kress, A.T. Laasanen, N. Leonardo, C. Liu, V. Maroussov, P. Merkel, D.H. Miller, N. Neumeister, I. Shipsey, D. Silvers, A. Svyatkovskiy, H.D. Yoo, J. Zablocki, Y. Zheng

Purdue University Calumet, Hammond, USA

N. Parashar

Rice University, Houston, USA

A. Adair, C. Boulahouache, K.M. Ecklund, F.J.M. Geurts, B.P. Padley, R. Redjimi, J. Roberts, J. Zabel

University of Rochester, Rochester, USA

B. Betchart, A. Bodek, Y.S. Chung, R. Covarelli, P. de Barbaro, R. Demina, Y. Eshaq, H. Flacher, A. Garcia-Bellido, P. Goldenzweig, Y. Gotra, J. Han, A. Harel, D.C. Miner, D. Orbaker, G. Petrillo, W. Sakumoto, D. Vishnevskiy, M. Zielinski

The Rockefeller University, New York, USA

A. Bhatti, R. Ciesielski, L. Demortier, K. Goulian, G. Lungu, S. Malik, C. Mesropian

Rutgers, the State University of New Jersey, Piscataway, USA

O. Atramentov, A. Barker, D. Duggan, Y. Gershtein, R. Gray, E. Halkiadakis, D. Hidas, D. Hits, A. Lath, S. Panwalkar, R. Patel, K. Rose, S. Schnetzer, S. Somalwar, R. Stone, S. Thomas

University of Tennessee, Knoxville, USA

G. Cerizza, M. Hollingsworth, S. Spanier, Z.C. Yang, A. York

Texas A&M University, College Station, USA

R. Eusebi, W. Flanagan, J. Gilmore, A. Gurrola, T. Kamon, V. Khotilovich, R. Montalvo, I. Osipenkov, Y. Pakhotin, A. Safonov, S. Sengupta, I. Suarez, A. Tatarinov, D. Toback, M. Weinberger

Texas Tech University, Lubbock, USA

N. Akchurin, C. Bardak, J. Damgov, C. Jeong, K. Kovitanggoon, S.W. Lee, T. Libeiro, P. Mane, Y. Roh, A. Sill, I. Volobouev, R. Wigmans, E. Yazgan

Vanderbilt University, Nashville, USA

E. Appelt, E. Brownson, D. Engh, C. Florez, W. Gabella, M. Issah, W. Johns, P. Kurt, C. Maguire, A. Melo, P. Sheldon, B. Snook, S. Tuo, J. Velkovska

University of Virginia, Charlottesville, USA

M.W. Arenton, M. Balazs, S. Boutle, B. Cox, B. Francis, J. Goodell, R. Hirosky, A. Ledovskoy, C. Lin, C. Neu, R. Yohay

Wayne State University, Detroit, USA

S. Gollapinni, R. Harr, P.E. Karchin, C. Kottachchi Kankamamge Don, P. Lamichhane, M. Mattson, C. Milstène, A. Sakharov

University of Wisconsin, Madison, USA

M. Anderson, M. Bachtis, J.N. Bellinger, D. Carlsmith, S. Dasu, J. Efron, L. Gray, K.S. Grogg, M. Grothe, R. Hall-Wilton, M. Herndon, A. Hervé, P. Klabbers, J. Klukas, A. Lanaro, C. Lazaridis, J. Leonard, R. Loveless, A. Mohapatra, I. Ojalvo, D. Reeder, I. Ross, A. Savin, W.H. Smith, J. Swanson, M. Weinberg

†: Deceased

1: Also at CERN, European Organization for Nuclear Research, Geneva, Switzerland

2: Also at Universidade Federal do ABC, Santo Andre, Brazil

- 3: Also at Laboratoire Leprince-Ringuet, Ecole Polytechnique, IN2P3-CNRS, Palaiseau, France
- 4: Also at Suez Canal University, Suez, Egypt
- 5: Also at British University, Cairo, Egypt
- 6: Also at Fayoum University, El-Fayoum, Egypt
- 7: Also at Soltan Institute for Nuclear Studies, Warsaw, Poland
- 8: Also at Massachusetts Institute of Technology, Cambridge, USA
- 9: Also at Université de Haute-Alsace, Mulhouse, France
- 10: Also at Brandenburg University of Technology, Cottbus, Germany
- 11: Also at Moscow State University, Moscow, Russia
- 12: Also at Institute of Nuclear Research ATOMKI, Debrecen, Hungary
- 13: Also at Eötvös Loránd University, Budapest, Hungary
- 14: Also at Tata Institute of Fundamental Research - HECR, Mumbai, India
- 15: Also at University of Visva-Bharati, Santiniketan, India
- 16: Also at Sharif University of Technology, Tehran, Iran
- 17: Also at Shiraz University, Shiraz, Iran
- 18: Also at Isfahan University of Technology, Isfahan, Iran
- 19: Also at Facoltà Ingegneria Università di Roma, Roma, Italy
- 20: Also at Università della Basilicata, Potenza, Italy
- 21: Also at Laboratori Nazionali di Legnaro dell' INFN, Legnaro, Italy
- 22: Also at Università degli studi di Siena, Siena, Italy
- 23: Also at California Institute of Technology, Pasadena, USA
- 24: Also at Faculty of Physics of University of Belgrade, Belgrade, Serbia
- 25: Also at University of California, Los Angeles, Los Angeles, USA
- 26: Also at University of Florida, Gainesville, USA
- 27: Also at Université de Genève, Geneva, Switzerland
- 28: Also at Scuola Normale e Sezione dell' INFN, Pisa, Italy
- 29: Also at University of Athens, Athens, Greece
- 30: Also at The University of Kansas, Lawrence, USA
- 31: Also at Institute for Theoretical and Experimental Physics, Moscow, Russia
- 32: Also at Paul Scherrer Institut, Villigen, Switzerland
- 33: Also at University of Belgrade, Faculty of Physics and Vinca Institute of Nuclear Sciences, Belgrade, Serbia
- 34: Also at Gaziosmanpasa University, Tokat, Turkey
- 35: Also at Adiyaman University, Adiyaman, Turkey
- 36: Also at The University of Iowa, Iowa City, USA
- 37: Also at Mersin University, Mersin, Turkey
- 38: Also at Izmir Institute of Technology, Izmir, Turkey
- 39: Also at Kafkas University, Kars, Turkey
- 40: Also at Suleyman Demirel University, Isparta, Turkey
- 41: Also at Ege University, Izmir, Turkey
- 42: Also at Rutherford Appleton Laboratory, Didcot, United Kingdom
- 43: Also at School of Physics and Astronomy, University of Southampton, Southampton, United Kingdom
- 44: Also at INFN Sezione di Perugia; Università di Perugia, Perugia, Italy
- 45: Also at Utah Valley University, Orem, USA
- 46: Also at Institute for Nuclear Research, Moscow, Russia
- 47: Also at Los Alamos National Laboratory, Los Alamos, USA
- 48: Also at Erzincan University, Erzincan, Turkey